

**LEARNING FROM HURRICANE IRMA, DIFFERENTIATING TSUNAMI FROM
HURRICANE DEPOSITS, AND RE-EVALUATING POSSIBLE TSUNAMI DEPOSITS
ON ST. THOMAS, US VIRGIN ISLANDS**

Final Technical Report

Research supported by the U.S. Geological Survey (USGS),
Department of the Interior, under USGS Grant No. G19AP00101

Principal Investigator, Martitia P. Tuttle
Co-Principal Investigator, Zamara Fuentes

M. Tuttle & Associates
P.O. Box 345
Georgetown, ME 04548
Tel: 207-371-2007
E-mail: mptuttle@earthlink.net
URL: <http://www.mptuttle.com>

Project Period: 8/1/2019-3/31/2021

Program Element I: Regional Earthquake Hazards Assessments

Key Words: Paleoseismology, Tsunami Geology, Age Dating

*The views and conclusions contained in this document are those of the authors and
should not be interpreted as necessarily representing the official policies, either
expressed or implied, of the U.S. Government.*

**LEARNING FROM HURRICANE IRMA, DIFFERENTIATING TSUNAMI FROM
HURRICANE DEPOSITS, AND RE-EVALUATING POSSIBLE TSUNAMI DEPOSITS
ON ST. THOMAS, US VIRGIN ISLANDS**

Principal Investigator
Martitia P. Tuttle

Co-Principal Investigator
Zamara Fuentes

M. Tuttle & Associates
P.O. Box 345
Georgetown, ME 04548
Telephone: (207) 371-2007
E-mail: mptuttle@earthlink.net

ABSTRACT

Overwash deposits resulting from Hurricane Irma's storm surge formed at five coastal study sites but only extended into Saba Pond on Saba Islet ~4.5 km south of St. Thomas. At Magens Bay, overwash deposits extended inland along a stream and probably into a ponded area, but the area was inaccessible due to debris from damaged mangroves. At Cabrita Pond on the northeast coast, two overwash fans composed primarily of lithic and carbonate cobbles reached the pond's edge but otherwise did not contribute to the pond bottom sediment. Sediment cores collected at Saba Pond and at Magens Bay, near the stream and ponded area, revealed that the overwash deposits are relatively thin, fairly well sorted, and composed primarily of carbonate sand. At Saba Pond, the deposit fines and thins inland in less than 10 m. Overwash deposits slightly deeper in the cores collected at Saba Pond and at Perseverance Pond, on the southern coast of St. Thomas, are thought to be related to the 1867 tsunami originating in Anegada Passage. These are sheet deposits that have sharp basal contacts and extend across the ponds. They are somewhat poorly sorted, normally graded, and composed of a mixture of carbonate sand, lithics, shells, and clasts of underlying deposits.

Through additional study and dating of sediment cores collected in 2020 and previously at the study sites, overwash deposits that share characteristics with tsunami deposits are recognized at multiple sites and are interpreted as resulting from three, possibly five, major overwash events. In addition to the 1867 tsunami, these events include (1) the A.D. 1800-1650 event also observed on Anegada, BVI, and probably the A.D. 1755 Lisbon tsunami, (2) the A.D. 1480-1200 event first recognized on Anegada and likely caused by a $M > 8$ earthquake generated by the Puerto Rico subduction zone or related faults north of the BVI, (3) an event in B.C. 390-890 that appears to have been as significant as the A.D. 1480-1200 event, and two less certain events in A.D. 200-B.C. 360 and B.C. 2350-3080. Dating during this study suggests that the age range of the A.D. 1480-1200 event can be narrowed to A.D. 1390-1280. Although age estimates of some of the overwash deposits still have large uncertainties, confidence in the interpretations of the deposits has been gained by comparing their characteristics with those of overwash deposits that formed during Hurricane Irma and the 1867 tsunami as well as other storms and tsunamis.

INTRODUCTION

Since the mega-thrust earthquakes of moment magnitude, $M > 9$ produced by subduction zones with no historical precedents, such as the events 2004 Aceh-Andaman, Indonesia, and 2011 Tohoku, Japan events, investigating subduction zones and related faults around the world has become a priority (e.g., Atlantic and Gulf of Mexico Tsunami Hazard Assessment Group, 2008; ten Brink et al., 2014; Hupers et al., 2017; Bilek and Lay, 2018). Following the 2004 Aceh-Andaman event, the Puerto Rico Trench (PRT) and the Lesser Antilles subduction zone in the northeast Caribbean were identified as a possible source of great earthquakes that could endanger the U.S. Atlantic coast as well as Puerto Rico and the Virgin Islands (PRVI) (Figure 1; ten Brink, 2005; ten Brink et al., 2014). The PRVI region has a history of destructive earthquakes some of which produced tsunamis; however, the locations and magnitudes of the historic earthquakes are poorly constrained (e.g., Reid and Taber, 1919; McCann, 1985; Figure 1). Furthermore, the earthquake potential and recurrence rates of offshore sources are essentially unknown (Mueller et al., 2003). Tsunami geology studies gather evidence of significant past events that can be used to reconstruct a longer record of earthquakes and to model the locations and magnitudes of offshore earthquakes (e.g., Rhodes et al., 2006). As demonstrated in the Pacific Northwest and in Alaska and northeastern Honshu, Japan, paleotsunami data has been used to estimate the timing and recurrence of mega-thrust earthquakes and can help to reduce uncertainty in earthquake hazard assessments (e.g., Minouri et al., 2001; Atwater et al., 2005; Kelsey et al., 2005; Namegaya et al., 2010; Nelson et al., 2006 and 2015).

In 2008, tsunami geology studies began on Anegada, British Virgin Islands (BVI), the closest island to the Puerto Rico trench (Figure 1). During the initial pilot study, large erosional scours of beach ridges as well as onshore deposits of broadly distributed layers of shelly sand capped by lime mud and carbonate cobbles and boulders, including coral heads, were attributed to a significant overwash of the island about A.D. 1650-1800 (Atwater et al., 2012; Reinhardt et al., 2012). Subsequent studies on Anegada found an earlier set of erosional scours of beach ridges, as well as many coral heads and a stratigraphically deeper shelly sand layer, resulting from a more significant overwash event about A.D. 1200-1480 (Atwater et al., 2017). The two overwash events were likely related to tsunamis given the similarity in scale of the Anegada erosional and depositional features with those that formed along the northwest coast of Japan during the 2011 tsunami, and not with those that formed during category 3-4 hurricanes that struck Anegada during the past 50 years (Atwater et al., 2014 and 2017). The 1755 Lisbon earthquake is the likely cause of the A.D. 1650-1800 overwash since the 1755 tsunami is known to have inundated other islands in the northeastern Caribbean. The Puerto Rico subduction zone or related faults north of the BVI is the preferred source of the more significant overwash that impacted Anegada circa A.D. 1200-1400. There is no known record in Western Europe of a tsunami that corresponds with this earlier event. Numerical modeling of the two events found that the A.D. 1650-1800 deposits could be caused by the 1755 Lisbon trans-Atlantic tsunami if the source model included a NNW-SSE fault rupture and $M 9.0$ earthquake (Wei et al., 2012). Modeling also found that the A.D. 1200-1480 deposits could be explained by either a $M \geq 8.4$ earthquake produced by thrust faulting on the Puerto Rico subduction zone or a $M \geq 8.2$ earthquake produced by normal faulting on the outer wall of the Puerto Rico trench (Wei et al., 2016). The deposits could not be explained by storm surge produced by category 4 and 5 hurricanes largely due to dissipation of wave energy by the reef and/or subtidal flats.

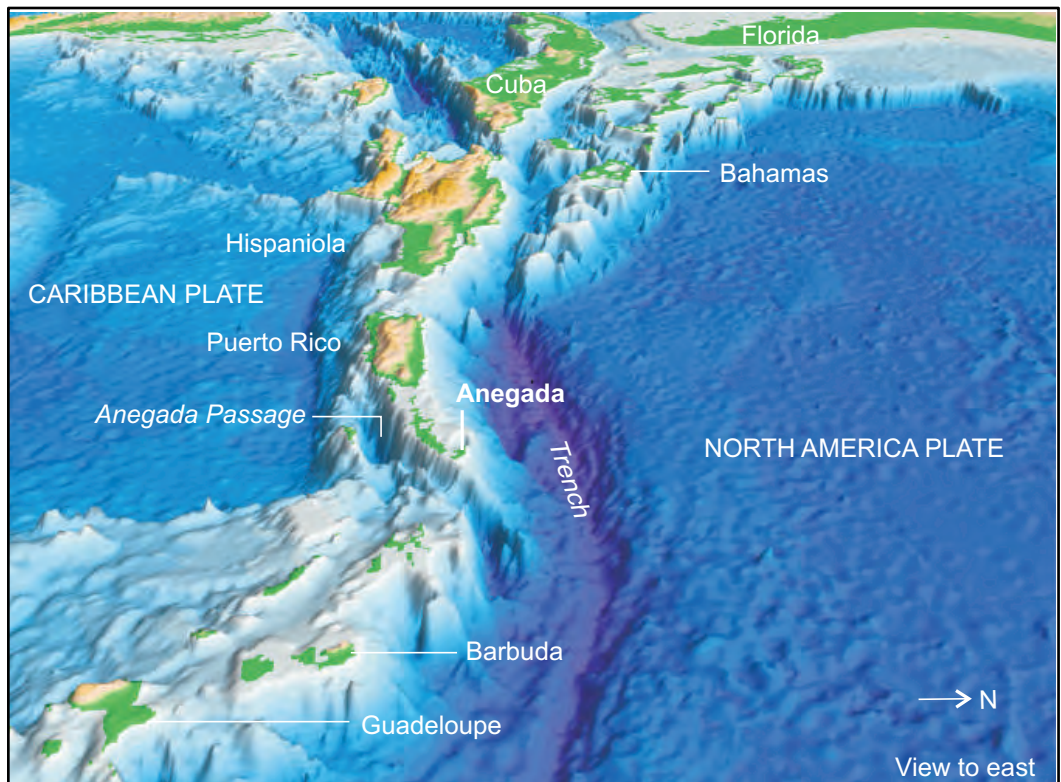
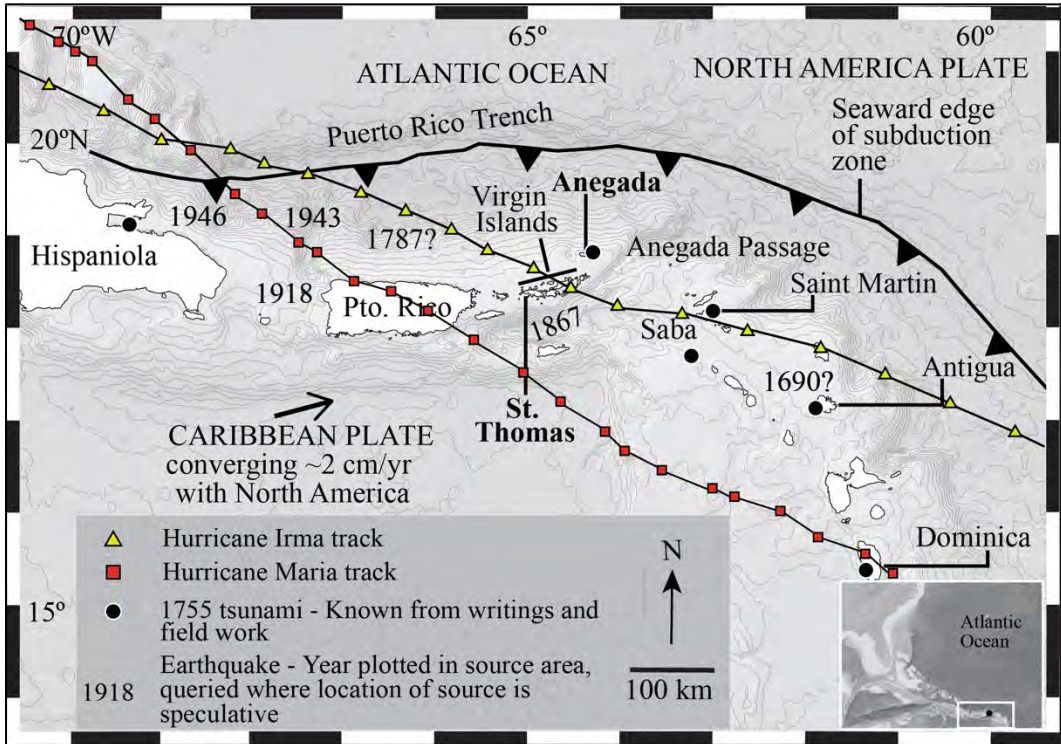


Figure 1. Tectonic plates and physiography of the northeast Caribbean. (Upper) Plan view showing large historical offshore earthquakes (year), plate convergence direction and rate (from López et al., 2006), observations of 1755 Lisbon tsunami (from O’Loughlin and Lander, 2003), and paths of 2017 Hurricanes Irma and Maria. (Lower) Oblique view westward.

The findings on Anegada prompted reconnaissance on St. Thomas, U.S. Virgin Islands (USVI), about 80 km southwest of Anegada and between Anegada and Puerto Rico (Figure 1). If the A.D. 1650-1800 and A.D. 1200-1480 overwash deposits on Anegada were indeed related to the 1755 Lisbon tsunami and a Puerto Rico subduction zone event, a sedimentological record of these events would likely in coastal ponds on other islands in the northeastern Caribbean. If a broader distribution of the A.D. 1650-1800 and A.D. 1200-1480 deposits were found, they could help to further constrain the seismic source models for the events. Coastal ponds on the northern and southern coasts of St. Thomas were selected for reconnaissance based on their locations with respect to historical and prehistorical tsunamis, potential to trap and preserve overwash deposits, and low anthropogenic disturbance.

Initial findings were promising and led to more detailed investigations including collection, descriptions, and analyses of sediment cores and radiocarbon dating of samples collected from the cores (Figures 2 and 3; Fuentes et al., 2017; Tuttle et al., 2017). Numerous shelly sand layers were identified in the sediment cores. Those interpreted as tsunami deposits exhibit sedimentological characteristics of modern tsunami deposits, including mixed composition of sediment derived from multiple environments of deposition, presence of broken shells and rip-up clasts, mixed or disturbed sediment, and coincidence with drastic changes to the environment of deposition (Table 1). Radiocarbon dating suggested that some of the likely tsunami deposits are similar in age to the A.D. 1650-1800 and A.D. 1200-1480 overwash deposits on Anegada and that there may be 2-4 prior events recorded at St. Thomas. In addition, a fairly young deposit in Perseverance Pond might on the southern coast might be related to the tsunami resulting from the 1867 $M \sim 7.3$ earthquake in the Anegada Passage (Figures 1, 2, and 3). Detailed descriptions of the site settings and pond deposits, including likely tsunami deposits can be found in Fuentes et al., 2017. Additional dating was recommended to better constrain the ages of the likely tsunami deposits, to confirm that some are contemporaneous with the Anegada deposits, and to improve estimates of the timing of the earlier events. Given the age of the sediment in some of the cores, coastal pond sediment on St. Thomas appeared to have the potential to extend our knowledge of large offshore earthquakes in the northeastern Caribbean back $\sim 5,000$ years.

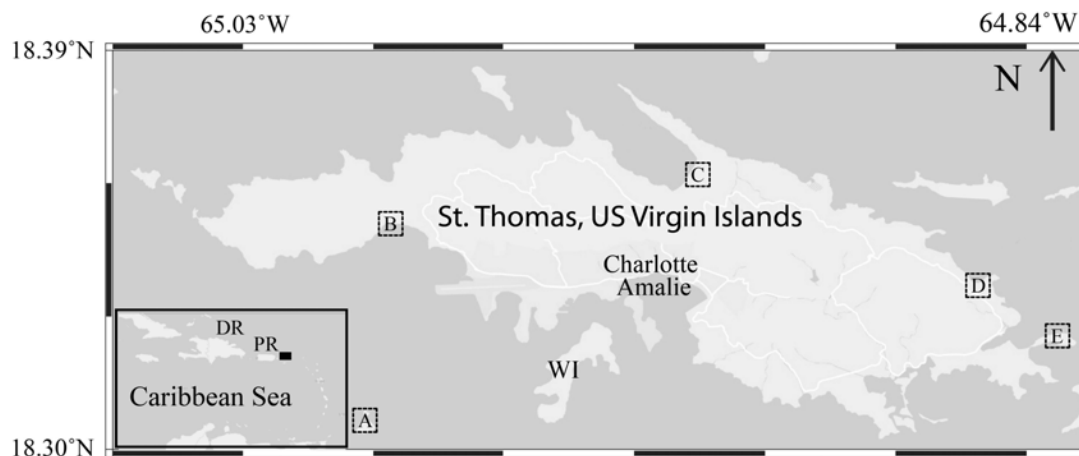


Figure 2. (A) Map of St. Thomas showing locations of study sites (stippled squares): (A) Saba Pond on Saba Islet ~ 4 -5 km south of St. Thomas, (B) Perseverance Pond (C) Magens Bay, (D) Smith Pond, (E) Cabrita Pond. WI denotes Water Island where wave height of the 1867 tsunami was ~ 12 m. Area of the map (black rectangle) is shown on the inset of the Caribbean. St. Thomas is located east of Puerto Rico (PR) and the Dominican Republic (DR) and northwest of the Lesser Antilles island chain.

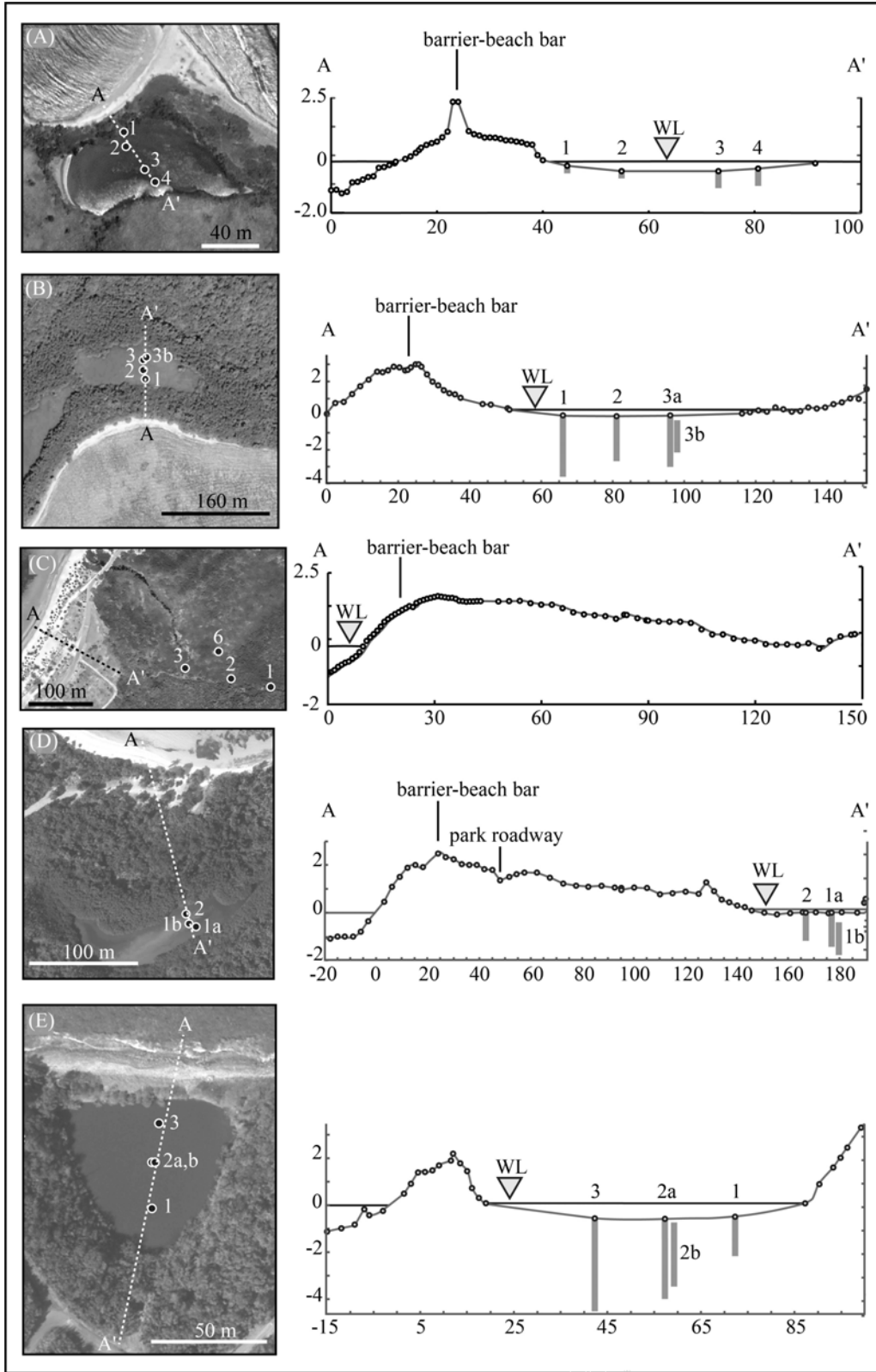


Figure 3. Study sites A, B, C, D, E whose locations are shown on Figure 2. (left) Satellite images showing core locations and transects; (right) topographic profiles along corresponding transects, showing pond levels (WL), core locations, and core depths.

Table 1. Characteristics of storm and tsunami deposits

Characteristic	Storm	Tsunami
Composition	Primarily reworked material from foreshore and backshore zones? ^{[2] [12]}	Mixed composition; sediment derived from multiple environments of deposition ^[2]
Biota	Mixture of diatoms, more brackish diatoms, not as broken ^[2]	Mixture of diatoms, but more likely to contain broken valves and benthic marine diatoms ^[2]
Sorting	Poor to well sorted ^[1] and well sorted ^{[3],[11],[12]}	Moderately-well sorted ^[1] and poorly sorted ^[3]
Grading	Normal or inverse grading ^[1]	Normal grading ^{[1],[2]}
Sedimentary and erosional structures	Interbedded with channels, multiple laminaset ^{[1],[2],[6]} , washover fans with parallel bedding and crossbedding ^{[2],[4]} , breaches swaths centimeters deep and a meter across ^[4] , massive ^[11]	Massive, single to few parallel beds ^{[1],[2],[12]} , breaches meters deep and tens of meters wide ^[4]
Rip-up clasts	Not present ^{[1],[3]} , reworked microbial mats ^[11]	Reworked clasts of underlying deposits present ^{[1],[2],[3]}
Bed thickness	Ranging up to 95 cm, thins inland ^{[1],[2]}	Rarely more than 25 cm ^{[1],[2]} , fills topographic lows ^[2] , usually thins landward ^[1] but can thicken landward locally ^[1]
Morphology	Overwash fans form inland of barrier bars and extend into ponds and streams ^{[2],[7]} , washover deposits thin inland ^{[2],[7]}	Sheet deposit ^{[1][3][4][7]}
Contacts	Vegetation buried in growth position by overwash deposit ^{[2],[3]}	Severed previous vegetation ^[2] , erosional ^[3]
Height above mean sea level	~1-2 m ^{[2],[4]} , >6m localized ^[6]	>4-10 m ^{[2],[7] [8]}
Landscape conformity	Does not advance beyond macrotopography ^{[1],[2],[6]}	Conform to previous landscape ^[1]
Inland extent	Tens of meters ^{[2],[4]} , hundreds of meters ^[6,10]	>1 km ^{[4],[9]}

Note: References in superscript brackets: 1-Goff et al., 2004; 2-Tuttle et al., 2004; 3-Morton et al., 2007; 4-Atwater et al., 2010; 5- Reicherter et al., 2010; 6-Goto et al., 2011; 7-Atwater et al., 2014; 8-Fukushima, 2015; 9-Nelson et al., 2015; 10-Kennedy et al., 2016; J; 11-Jamison-Todd et al., 2020; 12-Pilarczyk et al., 2021.

Historical Earthquakes, Tsunamis, and Hurricanes

The PRVI region has a long history of destructive earthquakes, including a moment magnitude, $M \sim 7.7$ event in 1943 located northwest of Puerto Rico, a $M \sim 7.5$ event in 1918 centered in the Mona Passage, a $M \sim 7.3$ event in 1867 in the Anegada Passage, a $M \sim 6.9-8.25$ event in 1787 whose location is still debated, and a $M \sim 6$ event in 1670 in western Puerto Rico (e.g., Reid and Taber, 1919; McCann, 1985; Mueller et al., 2003; Flores et al., 2012; Figure 1-upper image). The 1867 Anegada Passage and 1918 Mona Passage events are known to have produced tsunamis that inundated the coasts of PRVI (e.g., Reid and Taber, 1919).

For the 1867 Anegada Passage event, there were accounts of tsunami inundation at sixty-one locations from Grenada (~ 760 km southeast of St. Thomas) to Jamaica ($\sim 1,190$ km west of St. Thomas). For St. Thomas, wave heights reached 6 m at Charlotte Amalie on the south coast and 12 m at Water Island ~ 5 km south of Charlotte Amalie (<https://www.ngdc.noaa.gov>; Figure 2). For the 1918 event, there were accounts of tsunami inundation at more than twenty locations from the Dominican Republic on Hispaniola to the BVI (Figure 1). Wave heights were 6 m along the west coast of Puerto Rico, and diminished towards the east where they were 0.45 m at Charlotte Amalie and 0.7 m at Tortola, BVI, located between St. Thomas and Anegada (Figure 1) (<https://www.ngdc.noaa.gov>). The M 8.5 1755 Lisbon, Portugal, earthquake, produced a trans-Atlantic tsunami that was observed at seventeen locations across the northeastern Caribbean from Dominica to Hispaniola, with a maximum wave height of 6.4 m at Saba (not Saba Islet off the southern coast of St. Thomas) about 190 km southeast of St. Thomas (Figure 1; <https://www.ngdc.noaa.gov>). There are no known accounts of the 1755 tsunami for St. Thomas, but it seems likely that the tsunami washed up on its shores given the observations at other islands in the region.

Tropical storms and hurricanes that form in the eastern Atlantic and move westward across the northeastern Caribbean are a common occurrence. Between 1852 and 2017, seventy-eight tropical systems have passed within 150 km of Charlotte Amalie, St. Thomas. Sixteen of the tropical systems were classified as major hurricanes (Category 3-5), six of which passed to the west of St. Thomas, subjecting its coasts to strong winds and storm surges (<https://coast.noaa.gov/hurricanes>). Coastal surges resulting from storms vary depending on the storm's trajectory, wind field, wind speed, pressure, and storm speed. Hurricanes Hugo and Marilyn are two modern hurricanes that caused storm surge at St. Thomas. In 1989, the eye of Hurricane Hugo, a category 4, passed 55 km west of Charlotte Amalie, where a NOAA tide gauge measured a water level of 0.594 m above Mean High High Water (MHHW) (<https://tidesandcurrents.noaa.gov/>). In 1995, Hurricane Marilyn's eye, a category 2, passed northwest of the island 10 km from Charlotte Amalie, where the same tide station registered 0.744 m above MHHW. The storm surges for these two hurricanes were much less than the 6 m wave height reported for the 1867 tsunami at Charlotte Amalie.

In 2017, two major hurricanes, Irma and Maria, wreaked havoc on the islands of PRVI. On September 6th, 2017, Irma passed ~ 25 km north of St. Thomas as a category 5 hurricane with winds speeds of 184 mph and gusts of 224 mph. On September 20th, Maria passed ~ 85 km southwest of the island as a category 4 hurricane with winds speeds of 152 mph and gusts of 184 mph. The Coastal Emergency Risks Assessment (CERA) group provided storm surge and wave predictions for Hurricanes Irma and Maria based on the Advanced Circulation and Storm Surge model (<http://nc-cera.renci.org/>). According to the predictions, Hurricane Irma was likely to have a bigger coastal impact than Hurricane Maria on St. Thomas. For Irma, water heights

(storm surge) of 0.5-1 m were predicted for most of the island with higher values of 1.5-3+ m along parts of the north coast. In addition, offshore wave heights were predicted to be 6-12 m along the north coast of St. Thomas and 6-8 m along the south coast. The observed water height at Charlotte Amalie gauging station was measured a bit over 0.3 m above sea level on Sept 6th just before the station went offline. During the storm, a gauging station ~22 km to the east at Lameshur Bay on the south shore of St. John measured a maximum water height of ~0.45 m above sea level. For Hurricane Maria, water heights (storm surge) of <0.5 m were predicted for most of the island. Offshore wave heights were predicted to be 1-3 m along the north coast and <1 m along the south coast. During Maria, the gauging station at Charlotte Amalie was still offline. The gauging station at Lameshur Bay on St. John measured a maximum water height of ~0.33 m above sea level on Sept 20th and then went offline the next day. Of the two hurricanes, Irma is more likely to have produced storm surge that topped barrier bars, transported sediment inland, and deposited overwash deposits in coastal ponds.

Storm and Tsunami Deposits

Storm and tsunami deposits both result from onshore transport of nearshore sediment and therefore share some characteristics. Since storm deposits are common in the coastal sedimentary record of the Caribbean, care must be taken not to misinterpret storm deposits as tsunami deposits (Peters and Jaffe, 2010). Several studies have compared modern and historical storm and tsunami deposits and identified distinguishing characteristics (Nanayama et al., 2000; Goff et al., 2004; Tuttle et al., 2004; Kortekaas and Dawson, 2007; Goto et al., 2015; Atwater et al., 2014). Many of the characteristics of the two types of deposits are summarized in Table 1. In general, tsunami deposits are often composed of one to several massive or graded beds of sediment from multiple environments, and include rip-up clasts and broken valves; whereas, storm deposits often are interbedded and exhibit parallel and cross bedding within sediment derived primarily from the foreshore and backshore zones. Also, tsunami deposits resulting from large offshore earthquakes tend to be more broadly distributed in their coastal extent than storm deposits. Depending on topography, tsunami deposits may extend farther inland and to greater heights above sea level than storm deposits. However, Typhoon Haiyan in 2013 exceeded the expected landward extent and runup heights for storms (e.g., Pilarczyk et al., 2016; Soria et al., 2016). Was this case an end member of the normal range of storms or a more extreme storm relate to recent climate change? Additional research is needed to further characterize the severity of storms and their onshore deposits during the Holocene.

Hurricane Irma in 2017 deposits have been studied on Anegada, BVI, and on the islands of Turks and Caicos. On Anegada, the storm deposits included overwash fans of well sorted, fine to medium carbonate sands with intertidal mollusks and laminated sand sheets (Pilarczyk et al., 2021). On Turks and Caicos, the storm deposits included washover fans and lag deposits. The washover fans were massively bedded and composed of very well sorted, medium oolitic sand with some skeletal fragments and small microbial mat intraclasts; while the lag deposits consisted of lithified Holocene sediment or microbial mat intraclasts. Rip-up clasts are often associated with tsunami deposits. In this case, however, the setting, including carbonate platform 6 km in length by 1.6 km wide, low slope ridges, and shallow and expansive microbial mat coverage, provided an ideal setting for waves and storm surge to scour and remove pieces of microbial mat and transport them with other material across the platform. Hurricane Irma also impacted St. Thomas, providing the opportunity to characterize storm deposits at our previous

study sites and to use the information to further evaluate overwash deposits in sediment cores collected at those sites.

METHODOLOGY

During this study, we focused on the effects of Hurricane Irma on several previously studied coastal pond sites and used that information as well as additional dating results to re-evaluate our interpretations of tsunami deposits. The study involved (1) review of pre- and post-hurricane imagery of the Saba Pond, Perseverance Pond, Magens Bay, Smith Pond, and Cabrita Pond study sites; (2) investigations of the Saba Pond, Magens Bay, and Cabrita Pond sites where storm surge appeared to have overtopped the barrier bars forming overwash fans; (3) descriptions of Hurricane Irma deposits in cores collected at the Saba Pond and Magens Bay sites, descriptions of likely tsunami deposits in cores collected at Saba Pond, and collection of samples for dating; (4) radiocarbon dating of organic samples by Beta Analytic, Inc. and Pb-210 and Cs-137 dating of sediment samples by Amy Corp and Teledyne; (5) and interpretation of the various analyses.

For the review of pre- and post- hurricane imagery, Google Earth imagery was used for Saba and Smith Pond study sites and Google Earth imagery (pre-event) and NOAA digital aerial photographs (post-event) (National Geodetic Survey, 2021) were used for Perseverance Pond, Magens Bay, and Cabrita Pond sites. The apparent line between beach-dune sand and inland vegetation or the “sand line” was mapped on pre- and post-imagery and the two generations of images overlain to identify possible overwash deposits. Based on the results of the review, Saba Pond, Magens Bay, and Cabrita Pond were selected for site investigations.

During the investigations of Saba Pond, Magens Bay, and Cabrita Pond, the effects of Hurricane Irma storm surge were described, photographed, and their locations measured with a hand-held GPS unit. At Saba and Cabrita Ponds, where overwash deposits appeared to extend into the pond, a new surface corer developed by LacCore as well as a Bolivia/Livingstone corer were used to collect cores of pond-bottom sediment. The surface corer is designed to collect core without disturbing the sediment-water interface. This is important since the Hurricane Irma deposits were very close to the sediment-water interface. The new surface corer and the Bolivia corer allowed for the collection of 7-cm-diameter cores in polycarbonate tubes; whereas, the Livingstone used a 5-cm-diameter steel tube from which the cores were extruded into acrylonitrile butadiene styrene (ABS) tubes while in the field. At Magens Bays, where storm surge had flowed up a creek and devastated the adjacent mangroves, the Livingstone corer was used to collect cores of floodplain sediment. At Saba Pond and Magens Bay, topographic profiles were measured roughly perpendicular to the shoreline using a Sokkia B40 automatic level mounted on an aluminum tripod and a 3.96 m leveling rod. Surveys extended from the nearshore across the barrier-beach bar and either across the pond to the inland hillslope at Saba or along the trend of the creek at Magens Bay. Previously topographic profiles had been measured at Perseverance, Smith, and Cabrita Ponds. The ocean water level available from Charlotte-Amalie tidal observation station (Station # 9751639) was used to provide vertical control for the surveys.

Following fieldwork, Saba and Cabrita Ponds and Magens Bay cores were shipped to LacCore at University of Minnesota for description, analysis, sampling, and preservation. As part of the initial core description, cores were logged using a GEOTEK multi-sensor core logger and an XYZ point sensor. Cores were then split and imaged using a GEOTEK Geoscan-III (see photographs of cores in the Appendix). For the Saba and Magens Bay cores, the lithologic

(color, composition, grading, thickness, contacts with adjacent units) and biologic characteristics (integrity of shells and grains, biological assemblages) of the sediment were described consulting smear slides if possible (e.g., Schnurrenberger et al., 2003). Depositional units were defined and represented on stratigraphic columns. Special attention was given to recent deposits related to Hurricane Irma. The new cores from Saba and Magens Bay were also interpreted in terms of possible tsunami deposits. Unfortunately, LacCore was closed due to Covid-19 before the new cores from Cabrita Pond could be described and interpreted.

To try to better constrain the ages of specific deposits at the study sites, organic samples were collected from the newly collected cores from Saba Pond and Magens Bay as well as cores from Perseverance and Cabrita Ponds collected in 2014 and stored at LacCore. Because the laboratory was closed to outside investigators due to the Covid-19, we identified organic material near contacts of possible tsunami deposits using digital photographs of the cores. A LacCore staff member then collected the samples and sent them to M. Tuttle & Associates. We then inspected the samples using a binocular microscope and selected a subset of samples for radiocarbon dating. The samples were sent to Beta-Analytic, Inc. for accelerator mass-spectrometry (AMS) radiocarbon dating. Radiocarbon ages were converted to calendar years using the Calib 8.2 calibration method and the IntCal20 northern hemisphere calibration curve (e.g., Stuiver et al., 2020; Reimer et al., 2020), except for one sample from a new Magens Bay core for which we used the 2-sigma calibrated date determined by Beta Analytic (Bronk Ramsey, 2009; Reimer et al., 2013).

In cores previously collected at Perseverance Pond, a deposit fairly high in the section is thought to be related to the 1867 tsunami associated with a $M \sim 7.3$ earthquake in the Anegada Passage (Figure 1). Similarly, a deposit fairly high in the cores from Saba Pond also might be related to the 1867 tsunami. If so, they would serve as examples of a local tsunami deposit associated with a large historical earthquake in the region for comparison with other coastal pond deposits. The possible 1867 tsunami deposits at Perseverance and Saba Ponds are too young to get useful age estimates with radiocarbon dating. Therefore, we used Pb-210 and Cs-137 dating to estimate the ages of the deposit. Again because of Covid-19, we were not able to sample the cores as planned. In the fall of 2020, LacCore staff sampled the upper portion of core 3A at Perseverance Pond and core 4 at Saba Pond for Pb-210 and Cs-137 dating and sent the samples to M. Tuttle & Associates. It was difficult to arrange dating of the samples during the pandemic due to lab closures. In late winter 2021, Amy Corp with Teledyne began analyses of the samples. At the time of this writing, the results and interpretation of the results have not yet been received. The findings will be incorporated into an article about this study later this year.

IMAGERY, FIELD, AND LABORATORY ANALYSES

Review of Pre- and Post-Hurricane Imagery

In our review of Google Earth pre-event satellite images and NOAA post-event aerial photographs, storm surge appeared to have had a greater impact on Saba Pond, Magens Bay, and Cabrita Pond than on Perseverance and Smith Ponds. At Saba, a significant amount of vegetation was removed from the barrier bar and overwash fans formed that extended at least several meters into the pond (Figure 4). At Perseverance Pond, the beachfront appeared to have been eroded in places and several overwash fans extended a few meters into the vegetation on the barrier bar; but the fans did not extend beyond the bar or get anywhere near the pond located more than 20 m farther inland (Figure 5). At Magens Bay, storm surge appeared to have eroded the barrier bar and to have transported sand inland, covering roads and extending tens of meters into vegetated areas. Also, mangroves appeared to have been badly damaged along a stream that drains into the bay (Figure 6). At Smith Pond, portions of the beachfront appeared to have been eroded and overwash fans formed immediately behind the barrier bar covering nearby roads but had no effect on the pond more than 100 m farther inland (Figure 7). At Cabrita Pond, several small overwash fans formed on the barrier bar two of which may have reached the pond, suggesting that storm surge overtopped the barrier bar but otherwise had little effect on the pond (Figure 8).

Since Hurricane Irma passed to the north of Anegada, the winds driving storm surge would have been out of the north and northwest. As forecast by the Coastal Emergency Risks Assessment (CERA) group, water heights (storm surge) of 0.5-1 m were predicted for most of the island with higher values of 1.5-3+ m along parts of the north coast. The actual water height was not measured during the worst of the storm because the one gauging station on St. Thomas in Charlotte Amalie went offline. Although it was farthest from the storm track, Saba Pond appeared to be most affected by Hurricane Irma. The pond has a northern aspect and therefore was subjected to Irma's wind driven storm surge. Also, located on an isolated islet, Saba Pond was especially vulnerable to storm surge. Perseverance Pond appeared to be the least affected by storm surge. The pond has a southern aspect and is located on the southern side of the island. Therefore, of all the sites, it was the most protected from Hurricane Irma's storm surge.

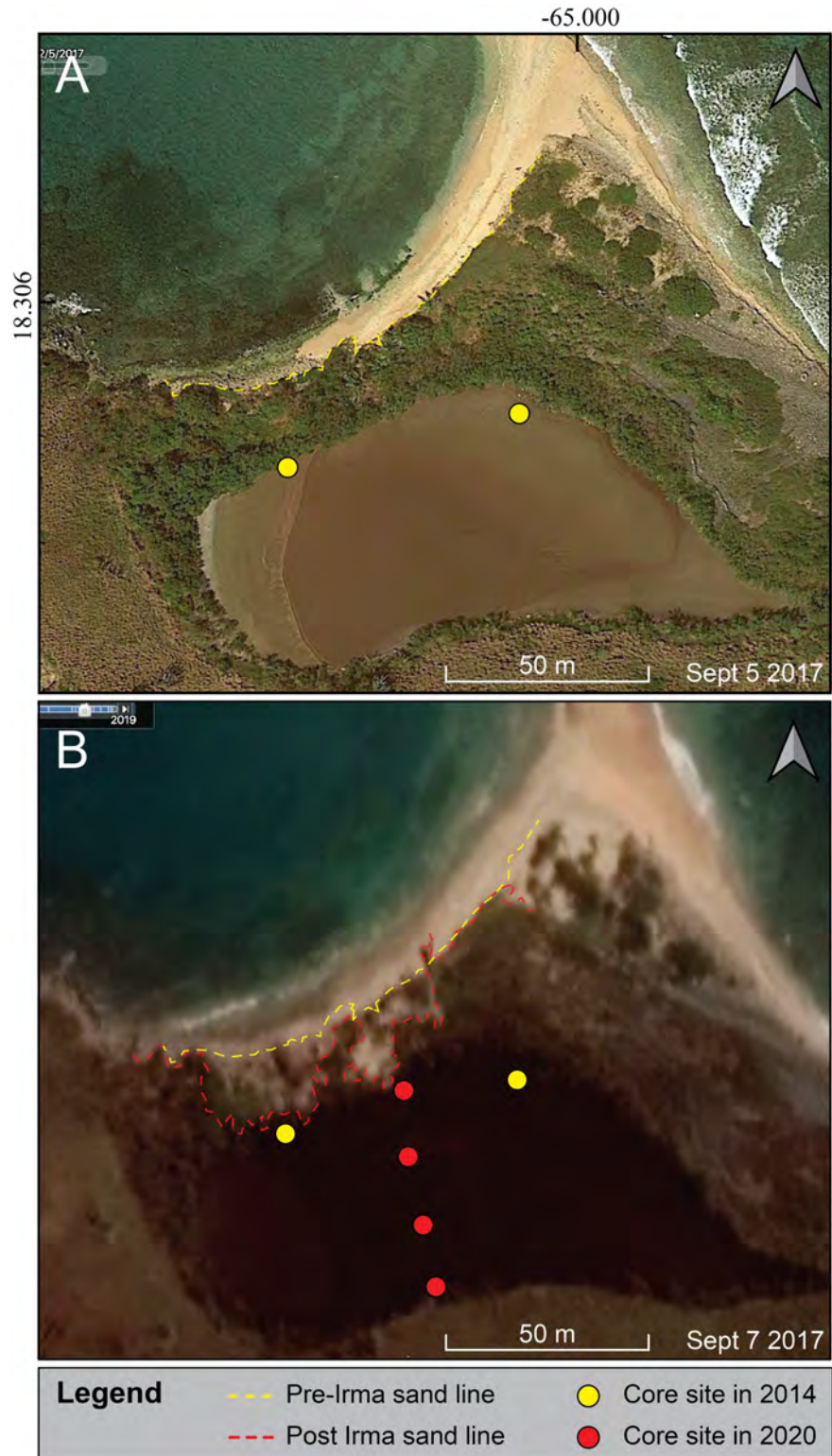


Figure 4. Before (A) and after (B) Hurricane Irma satellite imagery of Saba Pond on Saba Islet south of St. Thomas (from Google Earth, 2017). On B, note removal of vegetation from the barrier bar and overwash fans that extend into the northwestern portion of the pond.

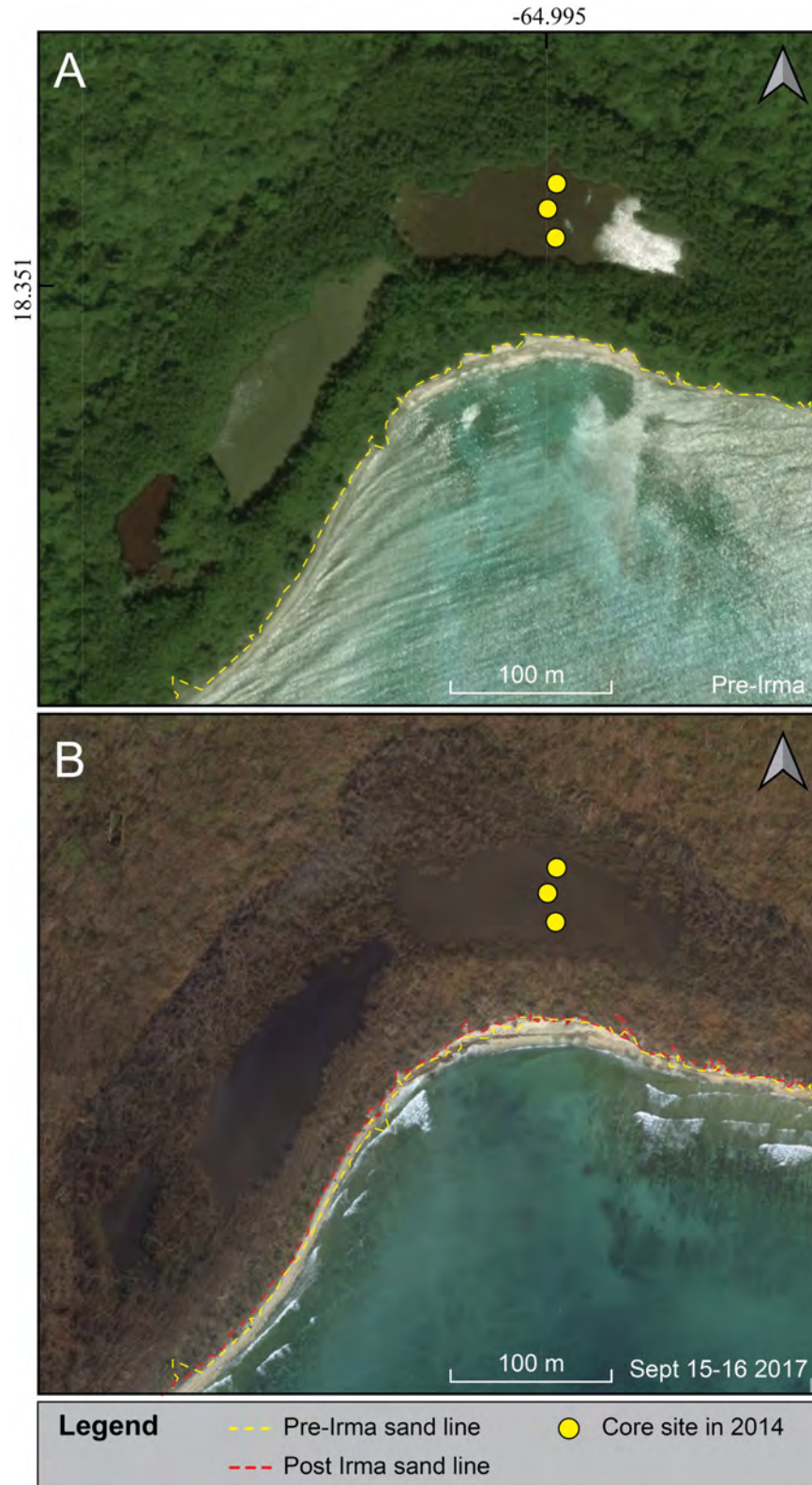


Figure 5. Before (A) and after (B) Hurricane Irma imagery of Perseverance Pond on St. Thomas (National Geodetic Survey, 2021). On B, note small overwash fans formed on the barrier bar effecting some vegetation but did not affect the pond more than 20 m farther inland.

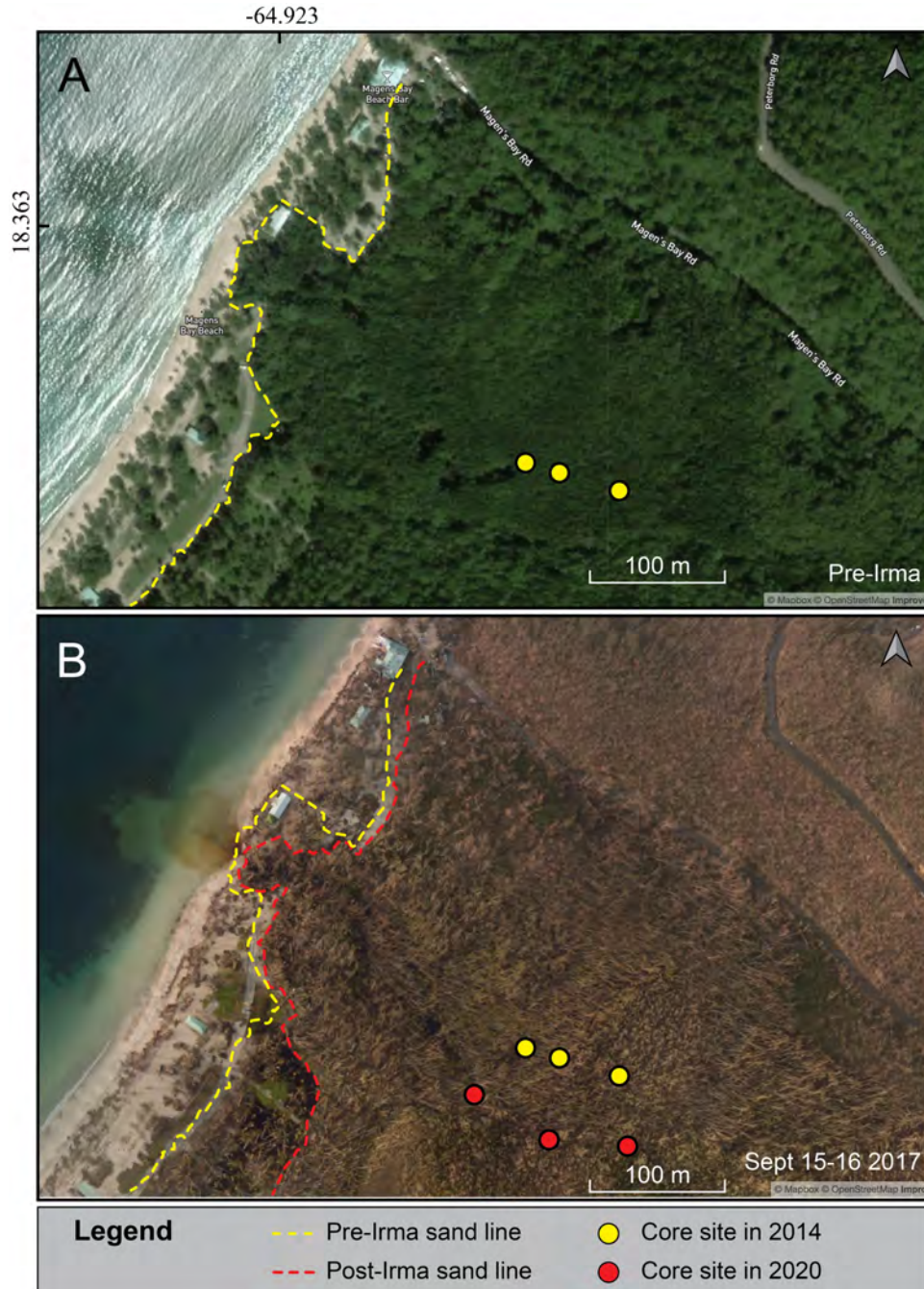


Figure 6. Before (A) and after (B) Hurricane Irma imagery of Magens Bay on St. Thomas (from National Geodetic Survey, 2021). Note overwash sand delineated by red line extends into vegetation behind the barrier bar and damaged mangroves occur along the course of a creek from which a dark plume discharges into the bay.

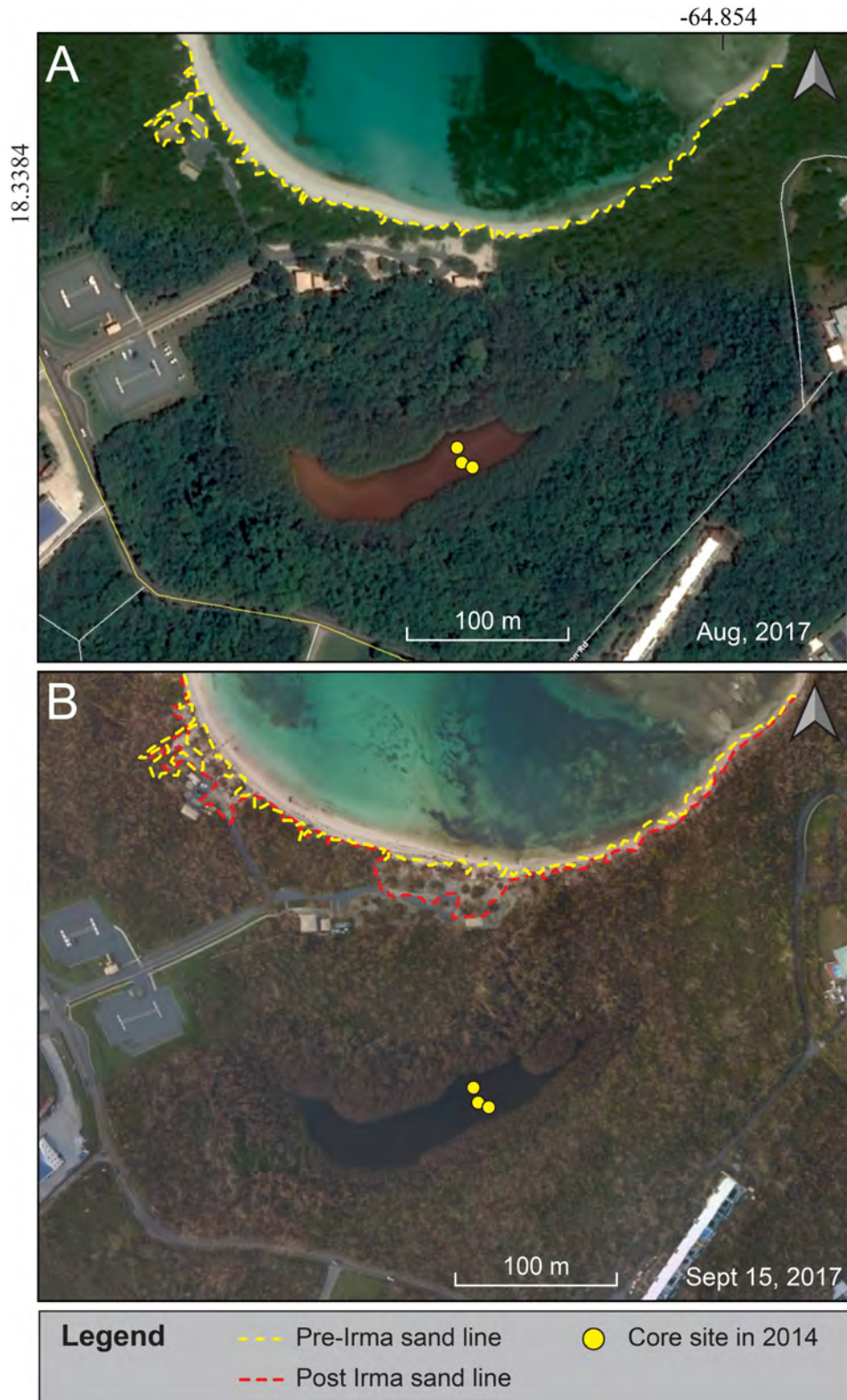


Figure 7. Before (A) and after (B) Hurricane Irma imagery of Smith Pond on St. Thomas (from National Geodetic Survey, 2021). On B, note several overwash fans extended inland of the barrier bar covering portion of roads but formed far from the pond.



Figure 8. Before (A) and after (B) Hurricane Irma imagery of Cabrita Pond on St. Thomas (from National Geodetic Survey, 2021). On B, note several small overwash fans formed in areas of previous fans and may have reached the edge of the pond but otherwise there appeared to be little effect on the pond.

Site Investigations

Site investigations at Saba Pond, Magens Bay, and Cabrita Pond involved ground truthing the areas where effects of storm surge were interpreted from pre- and post- Hurricane Irma imagery, documenting effects including overwash fans, and collecting and examining cores for those ponds where Hurricane Irma overwash deposits extended into the ponds. Site investigations were not conducted at Perseverance and Smith Ponds because our review of pre- and post-hurricane imagery indicated that Hurricane Irma overwash deposits formed nowhere near the ponds. Newly collected cores at Saba Ponds and Magens Bay were also examined to gain more information about older overwash deposits at the sites.

Saba Pond

At Saba, we surveyed the N60E oriented 100-m-long barrier bar along the northwestern side of the pond where effects of Hurricane Irma storm surge were the greatest (Figure 9). The ~2.3 m-high bar is characterized by coarse to fine sands with scattered cobbles along its northeastern section and mostly cobbles and scattered boulders along its southwestern section. Effects of storm surge included dead shrubbery in which there was some new growth, a large, uprooted sea-grape tree, wrack lines of organic debris, boulders, stacked cobbles, and overwash fans (Figure 9 and Table 2).

The overwash fans varied in morphology and size, and most were overgrown by sea purslane and crab grass at the time of our investigation 2 years and 5 months after the hurricane. Overwash fans that formed along the southwestern section of the barrier bar were composed of carbonate cobbles and carbonates, were narrow and elongated, and did not reach the pond. The overwash fans that formed along the central-northeastern section of the bar were composed mostly of sand with some carbonate cobbles. One of the most prominent fans extended into the pond about 3 meters (Figure 9- location 14). This fan ranged from moderately sorted, medium to coarse carbonate sands, with several scattered cobbles along its northeastern margin to poorly sorted, medium to coarse sands topped by carbonate cobbles and a wrack line of palm leaves and other vegetation along its southwestern margin.

Cores were collected at four locations along a roughly north-south transect across the pond (Figures 4 and 9). Core 1 was collected adjacent to the overwash fan at location 14 and clearly captured Hurricane Irma overwash deposit in the top of the core (Figure 10 – overwash deposit S-g; see Appendix for photographs of cores). The deposit also was found in cores 2 and probably in 4. It was not seen in core 3 because the upper portion of the section appeared to be missing in this location. The overwash deposit thins inland, from 4 cm at site 1 to an average of 1 cm at sites 2 and 4. At site 1, the deposit is characterized by gray, coarsening upward medium to coarse carbonate sand. With closer inspection using smear slides, the lower part of the deposit is composed of very well sorted, subangular to subrounded grains, with >50% undifferentiated carbonate grains of coarse sand size and <1% carbonate shell fragments (Figure 11). The upper part of the deposit is composed of moderately well sorted, subangular to rounded grains, with >50% undifferentiated carbonate grains of fine sand to very coarse sand size, 2% opaque minerals and <1 % carbonate shell material. In cores 2 and 4, the overwash deposit is characterized by gray, poorly sorted, mostly fine to medium carbonate sands. In summary, the Hurricane Irma overwash deposit is composed of very well sorted and coarsening upward medium to coarse carbonate sand with a few lithics and shell fragments. The deposit thins inland

from 4 cm near the barrier bar to ~1 cm within 10 m and becomes a moderately well sorted fine to medium carbonate sand.

During a reconnaissance visit to the pond in 2012, we found fragments of coral species *Acropora palmata*, *Orbicella annularis*, and *Diploria cavernosa* within the tangle of mangrove roots along the barrier bar and as part of an overwash fan that entered the pond from the north (Fuentes, et al., 2017). In Dutch spoon samples collected along the northern margin of the pond, we found two shelly overwash deposits that we interpreted as possible tsunami deposits. The lower 15 cm-thick deposit was composed of carbonate grains, clastic material, Halimeda fragments, and quartz grains. The upper 20 cm-thick deposit had an erosional basal contact and was composed of normally graded clastic material, including coarse to fine lithics, Halimeda fragments, and quartz grains. Mixed composition and normal grading of the deposits, and erosional basal contact for the upper deposit are all characteristics consistent with a tsunami origin (Table 1). Dating suggested the upper layer may have been deposited during the A.D. 1200-1480 tsunami while the lower layer might be related to an earlier event.

The cores collected in 2020 provide the opportunity to further evaluate possible tsunami deposits in Saba Pond. As expressed in the longest core, 4, there are four overwash deposits that are likely to be tsunami deposits, S-c, S-d, S-e, and S-f (Figure 10; see Appendix for photographs of cores). Unit S-c overlies a light-brown massive soil mixed with medium to coarse carbonate sand and various gastropod shells. S-c is characterized by a sharp basal contact and two fining upward layers of sand, possibly representing two pulses, in cores 3 and 4 (Figure 12). The lower layer is characterized by a poorly sorted mixture of carbonate and lithic material with gastropods and silt clasts that fines upward to a brown silt with gastropods and a few carbonate grains. The upper layer is characterized by medium to fine lithic sand with some carbonate grains that fines upward to fine lithic sands with layering of heavy minerals. The lithic sands contain gastropods and flat-lying leaves and grades into a cream-colored massive carbonate silt. In core 4, the unit is overlain by a light brown carbonate silt. Unit S-d is characterized by a sharp erosional basal contact and two fining upward layers of sand in cores 3 and 4. The lower portion of the couplet consists of a very poorly sorted mixture of carbonate grains, shell fragments, organic matter and lithic material. The upper portion of the couplet consists of medium carbonate sand with a few organic fragments that fines upward to gray carbonate silt. The top of the unit occurs in the bottom of core 2 as well as in cores 3 and 4 and is overlain by a massive medium brown to gray well-sorted organic silt with burrowing tracks. Unit S-e also has a sharp basal contact and is characterized by a massive light-brown very coarse sand that fines upward to gray silt. The lower portion of the unit is composed of lithics, carbonate grains, seeds, carbonate shells, and ostracod shells and thins inland from 5.5 cm in core 2 to 0.5 cm in core 4. The upper portion of the unit consists of silt-sized carbonates, lithics, and seeds concentrated near the top of the deposit. This unit occurs in all four cores and is overlain by a massive cream medium to coarse silt with a few grains of fine sands. Unit S-f has a sharp basal contact and consists of somewhat poorly sorted, carbonate sand with some heavy minerals, lithic grains, ostracod shell fragments, fine-sand-size foraminifera, and organics, that fines upward from very coarse to medium grains in core 1 and fines inland to fine and very fine grains in cores 2 and 4, respectively. The unit is overlain by black organic material that appears to be compacted extracellular polymeric substances, EPS, resulting from microbial activity. The units identified as likely to be tsunami deposits all have a sharp, sometimes erosional, basal contacts, are composed of one or two fining upward layers of mixed materials, including carbonate grains, lithics, shells, and clasts, and span most if not the entire width of the pond (Table 1; Figure 12).



Figure 9. Survey of Saba Pond showing locations (1-17) of effects of Hurricane Irma. (A) GE image acquired in November 2019 with indicated observation locations made in March 2020. (B) Southwest margin of sandy overwash fan extending into pond (location 14). (C) Back of overwash fan, showing wrack line, cobbles and boulders on top of sand and against a black mangrove (0.5 m shovel for scale) (location 14). (D) Southwest view of cobble and boulder deposit on southwest section of barrier bar (location 8). (E) Debris parallel to beach and lying against wild grape tree on southwest section of bar (location 10). (F) Northeast view along beach bar (pond to right) (location 11). (G) Southwest view of cobbly, overwash deposit (location 11).

Table 2. Effects of Hurricane Irma at Saba Pond on Saba Islet

Location ID No.	WP	Latitude	Longitude	Photo No.	Observations
1	256	N 18 18.417	W 65 00.024		Vegetation edge, new cover
2	258	N 18 18.406	W 65 00.037	178 182 184 185	New ground cover Wrack line Wrack line against tree Sand below ground cover
3	259	N 18 18.403	W 65 00.041		Top of bar
4	260	N 18 18.401	W 65 00.039	192	Back of bar
5	261	N 18 18.399	W 65 00.042	195	Wrack line
6	262	N 18 18.402	W 65 00.042		Overtured dead tree
7	263	N 18 18.399	W 65 00.047		Edge of vegetation
8	264	N 18 18.399	W 65 00.049		Fan of cobbles and boulders
9	266	N 18 18.397	W 65 00.054	196	Wrack line
10	267	N 18 18.395	W 65 00.057	198	Finger-like structure of cobbles
11	268	N 18 18.397	W 65 00.061		Wrack line? Suspicious
12	269	N 18 18.397	W 65 00.069		Exposed boulders and cobbles on top of bar
13	270	N 18 18.398	W 65 00.076	203	High point of bar, drifted wood
14	277	N 18 18.395	W 65 00.034		Location core 1
15	279	N 18 18.390	W 65 00.032		Location core 2
16	308	N 18 18.381	W 65 00.027		Location core 3
17	309	N 18 18.377	W 65 00.026		Location core 4

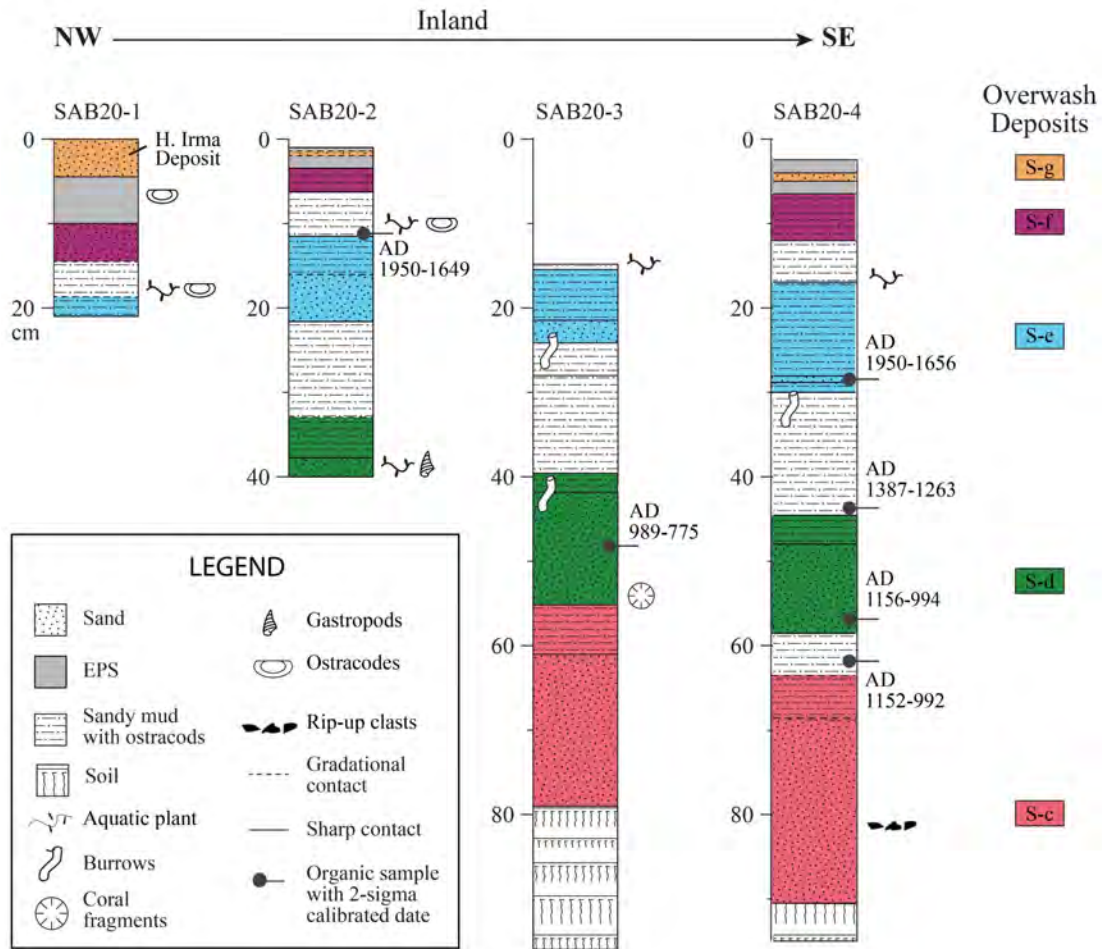


Figure 10. Stratigraphic columns based on interpretation of sediment cores collected at Saba Pond in 2020 (see Appendix for photographs of cores). Hurricane Irma overwash deposit (S-g), clearly captured in core 1, thinned abruptly between core 1 and 2 and appears to have extended across most of the pond to core 4. Overwash deposits S-c, S-d, S-e, and S-f are interpreted as likely tsunami deposits. EPS=extracellular polymeric substances resulting from microbial activity in shallow-water carbonate environments.

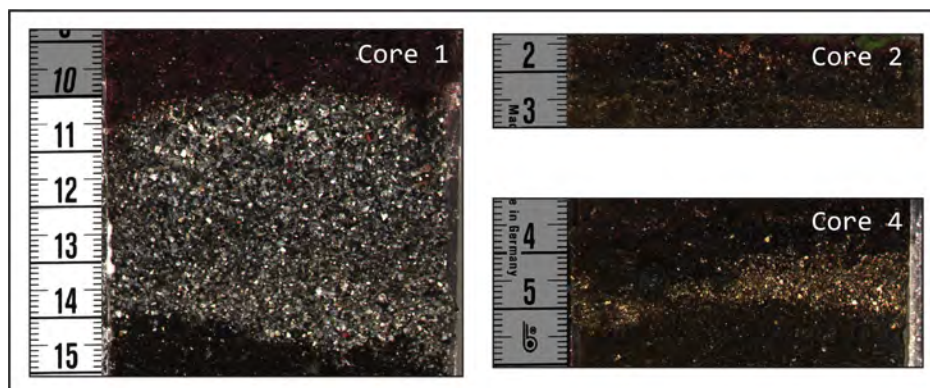


Figure 11. Photographs of Hurricane Irma's overwash deposit (S-g) in the upper portions of cores 1, 2, and 3 collected at Saba Pond. The deposit thins inland from 4 cm to 1 cm and fines inland from medium to very coarse carbonate sand in core 1 to fine to medium carbonate sand in core 4. Also, the storm deposit in core 1 contains more heavy minerals than it does in cores 2 and 4.

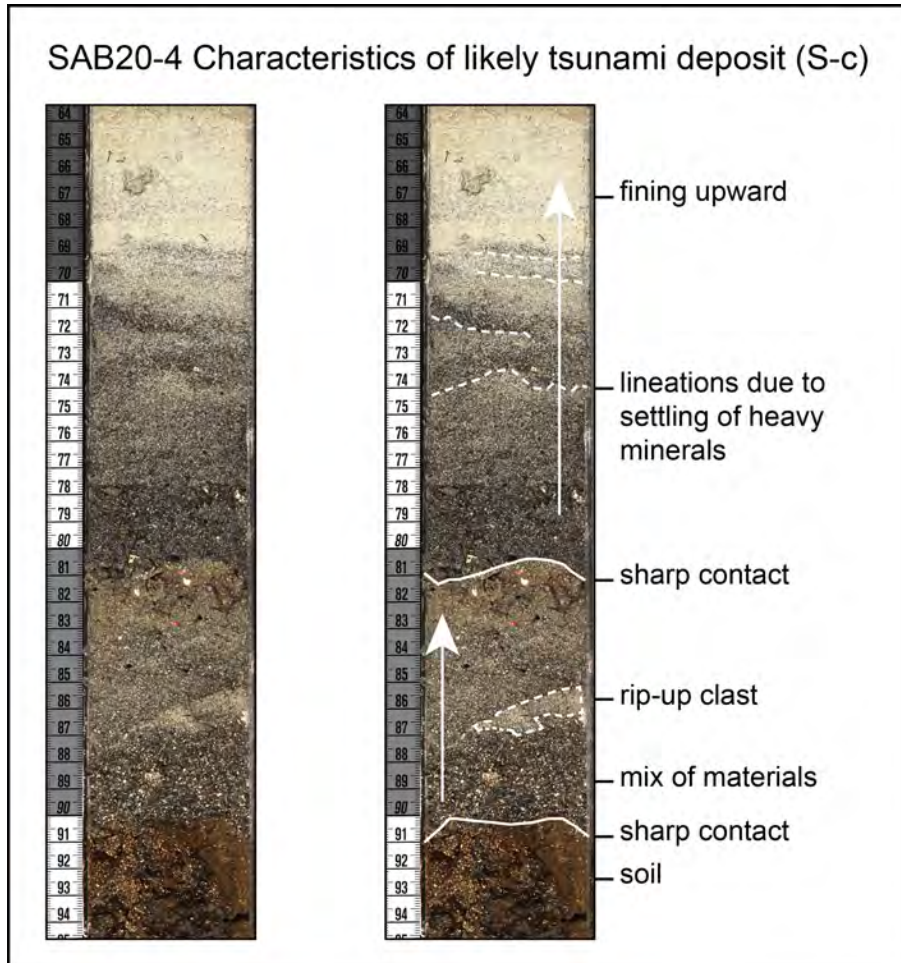


Figure 12. Unannotated (left) and annotated (right) photographs of overwash deposit S-c interpreted as a likely tsunami deposit. The deposit is characterized by a sharp basal contact, two fining upward layers of poorly sorted mixed materials including carbonate sands and silt, heavy minerals, lithic grains, gastropods and silt clasts.

Magens Bay

Magens Bay beach is a park that has been developed to accommodate several structures or sheds and two roads with parking areas along the length of the beach. A stream originating in the hills to the southeast flows through an area of mangroves to the beach. At times, the stream has been blocked by beach deposits, leading to the formation of a ponded area within the mangroves. During periods of high rainfall, the stream can break through the barrier bar to the bay. In 2012, we examined sediments in the ponded area using a Dutch spoon.

After interviewing park personnel about the effects of Hurricane Irma, we surveyed along the N38E oriented 1-km-long barrier bar, portions of the coastal plain, and along a trail subparallel to the stream (Figure 13 and Table 3). It appeared that vegetation along the beach front had been badly damaged and the area was recently replanted. The road closest to the beach was still covered with overwash sand and remained closed to vehicular traffic. Otherwise, most of the overwash deposits and damaged vegetation had been cleared and piled up near the tree line by the Magens Bay Authority.

We tried to access the ponded area along the creek to collect cores, but the 2+-m-high tangled debris from damaged mangroves was impenetrable. We collected cores at three locations along a N60W transect and adjacent to the mangrove area (locations 18, 19, and 20 on Figure 13). Core 3, collected ~250 m inland from the barrier bar and close to the stream, was the only core that captured Hurricane Irma's overwash deposit (Figures 14 and 15; see Appendix for photographs of cores). At that location, the deposit is a thin, ~1 cm, carbonate sand beneath the leaf litter and overlying a thin soil. With closer inspection using smear slides, the deposit is characterized by moderately well sorted, very angular to subrounded carbonate sand composed of >50% undifferentiated carbonate grains, 5% foraminifera and diatoms, and 1% siliceous biogenic components. The texture of the deposit ranges from medium size sand to clay with the coarser portion being composed of undifferentiated carbonate grains and the finer portion being composed of undifferentiated carbonate clayey silt, foraminifera, diatoms, and siliceous biogenic components.

During reconnaissance in 2012, we collected Dutch spoon samples in the ponded area along the stream and found two overwash deposits that might be related to tsunamis (Fuentes et al., 2017). The lower deposit, 72-90 cm below the surface, was a carbonate sand with shells and lithics in which a soil had developed. The upper deposit, 10-38 cm below the surface, was composed of multiple layers of carbonate sand with lithics and shells, including bivalves, gastropods, and shell fragments. Radiocarbon dating of a wood fragment (MB6-W2-76) within the upper 4 cm of the lower deposit, probably the soil, yielded a 2-sigma calibrated date of A.D. 1445-1396 and A.D. 1341-1329, providing a minimum constraining age of A.D. 1445 and suggesting the deposit may be related to the A.D. 1200-1480 tsunami. Dating of a leaf (MB6-W1-62) collected 24 cm below the upper deposit gave a calibrated date of A.D. 1630-1571, A.D. 1562-1559, and A.D. 1523-1441 providing a maximum constraining age of A.D. 1441 for the upper deposit. The maximum constraining age of the upper deposit suggests that it is historical in age and may have resulted from the A.D. 1800-1650 event.

The cores collected in 2020 provide the opportunity to further evaluate possible tsunami deposits at Magens Bay. As expressed in the longest core, 2, there are two overwash deposits, MB-d and MB-e (Figure 14; see Appendix for photographs of cores), that may be related to the overwash deposits in the nearby ponded area previously attributed to the A.D. 1200-1480 and A.D. 1800-1650 events. Unit MB-d observed from 73-112 cm below the surface in core 2 is a poorly sorted, light-brown, coarse to medium carbonate sand that fines upward to a gray sandy mud in which a soil developed in the upper 4-5 cm. The coarser lower portion of the unit is composed of 50% undifferentiated carbonates, 49% very angular to rounded *Halimeda* plates, and 1% siliceous biogenic components with several dark-green domains of an unidentified mineral covered with framboidal pyrite crystals. The finer portion of the unit is very fine carbonate sand, undifferentiated carbonate mud, and siliceous biogenic mud. Unit MB-e, from 4-40 cm below the surface, has a sharp basal contact in core 2 and is composed of bioturbated silty, fine to medium carbonate sand with lithics, shells, and few organics. The portion of MB-e captured in core 3 is also bioturbated, as is the entire depth of core 1, located farther from the stream and in crab territory, making correlation with units in this core more uncertain.



Figure 13. Survey of Magens Bay showing locations (1-21) of effects of Hurricane Irma. (A) GE image acquired in April 2019 with indicated observation locations made in March 2020. (B) View from bridge looking northwest towards beach. Dead mangroves still litter creek channel (location 21). (C) View from bridge towards southeast, dead mangroves flank channel (location 21). (D) North-northeast view up closed road covered with sand (right side). Beach front with new planted vegetation (location 10). (E) Mangrove area near trail, surveyed for coring (backpack for scale) (location 2). (F) Mangrove area showing burrowing by crabs; therefore, lower and inundated areas were targeted for coring instead (scale=20 cm) (location 2). (G) Area in vicinity of coring site, older mangroves were toppled and killed by storm surge and wind. New mangroves are starting to grow in their place (location 20).

Table 3. Effects of Hurricane Irma at Magens Bay on St. Thomas

Location ID No.	WP	Latitude	Longitude	Photo No.	Observations
1	250	N 18.36081	W 064.92307		Trail entrance
2	252	N 18.36092	W 064.92092		Tried to core but hit a root Concrete mark (5-U)
3	314	N 18 21.637	W 64 55.475		Shed #4
4	316	N 18 21.541	W 64 55.472		Mound of sand-from cleanup efforts
5	317	N 18 21.545	W 64 55.526		Limit sand reaching farthest inland
6	318	N 18 21.528	W 64 55.551		Entrance to Arboretum- gated
7	319	N 18 21.552	W 64 55.551		South gate
8	320	N 18 21.564	W 64 55.550		Limit of vegetation in front of parking lot.
9	321	N 18 21.576	W 64 55.560		End of tree line going towards beach
10	322	N 18 21.576	W 64 55.539		Gate to closed road, parallel to beach
11	323	N 18 21.588	W 64 55.465		Sand surrounding fallen but alive Ucar tree
12	324	N 18 21.639	W 64 55.434		Tall palm-tree
13	338	N 18 21.810	W 64 55.361		Shed #2
14	339	N 18 21.830	W 64 55.353		Restaurant and bar
15	340	N 18 21.839	W 64 55.332		Entrance
16	342	N 18 21.900	W 64 55.315		
17	343	N 18 21.900	W 64 55.298		Road in front of shed #1
18	253	N 18 21.652	W 64 55.244	161-162	Location core 1
19	254	N 18 21.652	W 64 55.280	177	Location core 2
20	337	N 18 21.667	W 64 55.322		Location core 3

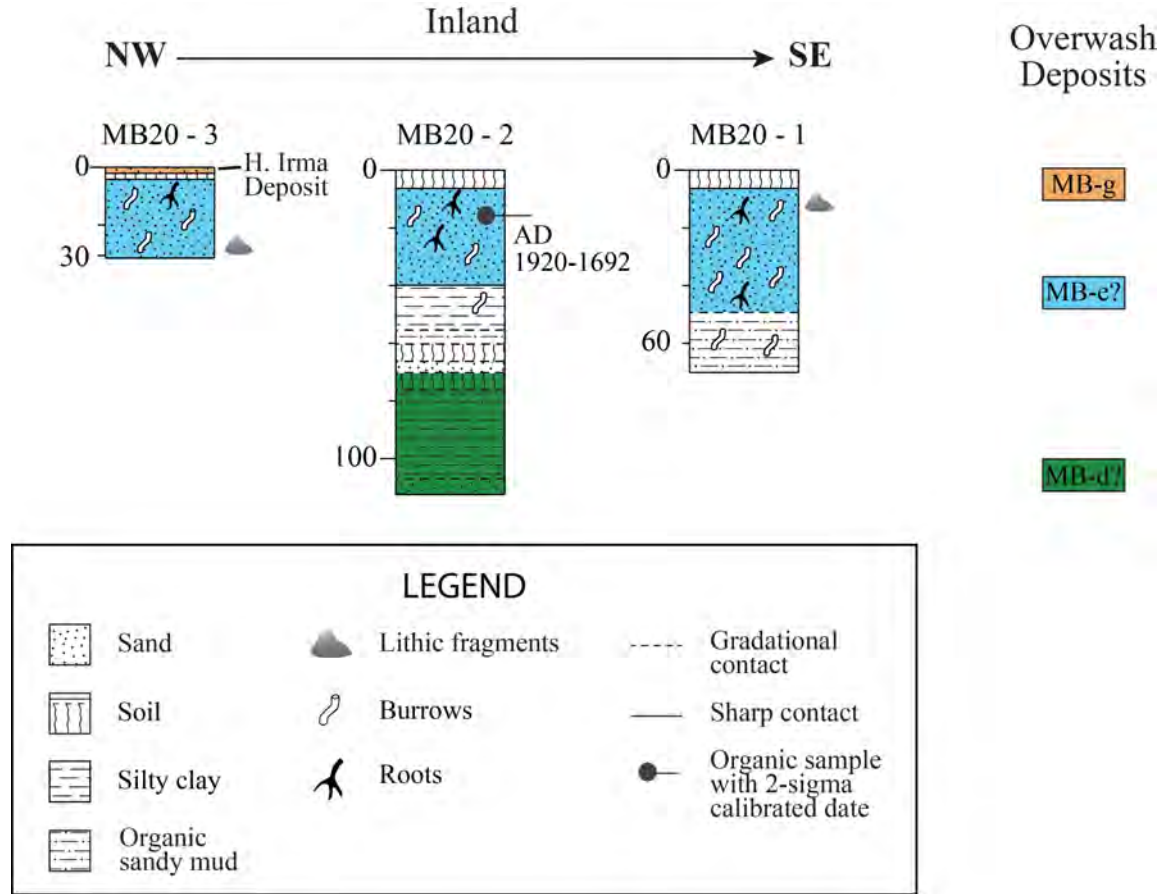


Figure 14. Stratigraphic columns based on interpretation of sediment cores collected at Magens Bay in 2020 (see Appendix for photographs of cores). Hurricane Irma overwash deposit, a thin carbonate sand beneath the leaf litter and overlying a thin soil, was found only in core 3 collected adjacent to the stream. Overwash deposits S-d and S-e, correlated with similar units observed previously in Dutch spoon samples collected in the nearby ponded area, are interpreted as likely tsunami deposits.

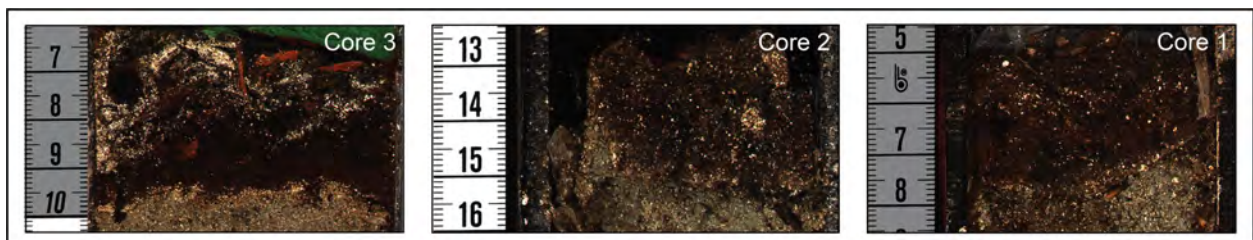


Figure 15. Photographs of the uppermost sediment in cores 1, 2, and 3 at Magens Bay. Hurricane Irma overwash deposit was only found in the upper portion of core 3. The deposit is poorly sorted and composed of medium carbonate grains with smaller amounts carbonate clayey silt, foraminifera, diatoms and siliceous biogenic components. The deposit was not observed in cores 2 and 3 collected farther inland.

Cabrita Pond

At Cabrita, we surveyed along the N90E oriented 130-m-long barrier bar north of the pond where effects of Hurricane Irma storm surge were the greatest (Table 4 and Figure 8). The ~2 m-high barrier bar is characterized by igneous and carbonate cobbles, with some carbonate boulders and pebbles (Figure 16). Effects of storm surge included areas of dead shrubbery in which there was some new growth, wrack lines of plastic, trash debris, driftwood, and overwash fans. The overwash fans were still exposed 2 years and 5 months after the hurricane. Local residents confirmed that the fans formed during Hurricane Irma.

Two of the overwash fans extended as far as the edge of the pond and were composed of igneous and carbonate cobbles and several boulders (Figures 8 and 16 C and D). The western fan at location 1 was ~4.6 m wide and composed of lithic cobbles and boulders (30x26 cm and 40x30 cm), subangular pebbles, coarse sands, and cobble-size coral heads of *Montastrea*, *Porites*, and *Acropora* (palmata species) likely reworked from the barrier bar. The eastern fan was not as wide as the western fan and was composed of lithic and carbonate cobbles, and was partially covered by a wrack line of sea fans, drift wood, and trash debris.

In the vicinity of the two overwash fans, Dutch spoons samples of the pond sediment were examined for a recent overwash deposit related to Hurricane Irma (Figure 16 F). There was no trace of such a deposit. Nevertheless, we collected cores at three locations along the same transect used for coring in 2014. The plan was to inspect the cores for any evidence of Hurricane Irma and also to further evaluate and date possible tsunami deposits identified in cores collected in 2014. At LacCore, the cores were inspected for Hurricane Irma overwash deposits and none were found. Unfortunately, LacCore was shut down due to Covid-19 before the cores could be described. The cores are stored at LacCore where they can be studied in the future.

Table 4. Effects of Hurricane Irma at Cabrita Pond on St. Thomas

Location ID No.	WP	Latitude	Longitude	Picture	Observations
1	NA	18.326772	-64.837041	278	Overwash fan
2	NA	18.326781°	-64.836682°	285	Overwash fan
3	346	18.326533°	-64.836800°	323	Core site 1A
4	347	18.326367°	-64.836817°	na	Core site 2A
5	348	18.326200°	-64.836867°	na	Core site 3A
6	349	18.326650°	-64.836766°	na	Core site 4A

NA=Not available.

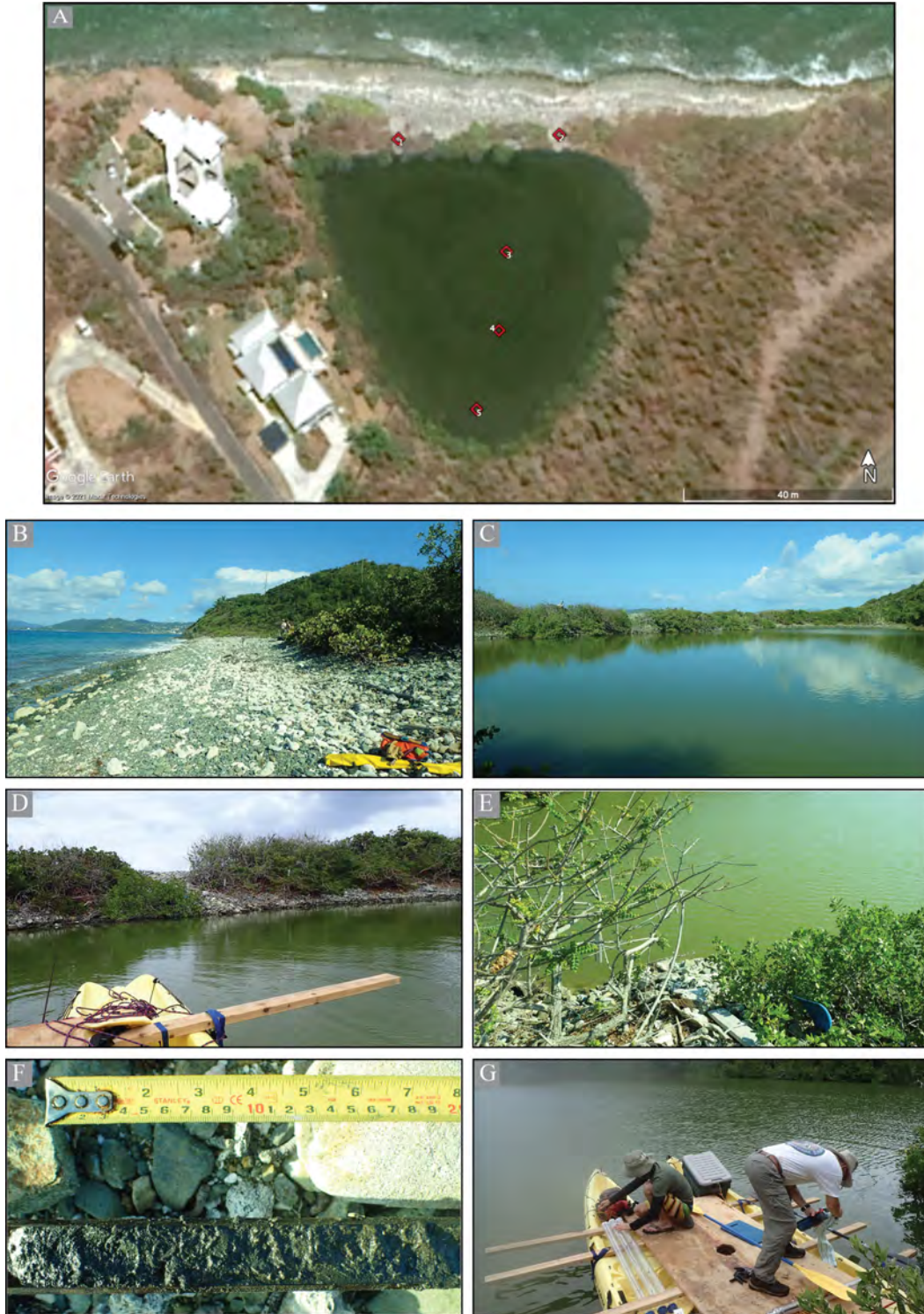


Figure 16. Survey of Cabrita Pond showing locations (1-5) of overwash deposits, or lack thereof, from 2017 Hurricane Irma. (A) GE image acquired in April 2019 with observation locations made in March 2020. (B) View east along the barrier bar (north of location 1). (C) View northeast from west margin of pond of fans at locations 1 and 2. (D) Closeup of easternmost overwash fan (location 2). (E) Wrack deposit on top of easternmost fan (location 2). (F) Dutch spoon core taken very close to location 2 - no overwash deposit is observed. (G) Preparing for piston coring in the pond.

Dating of Overwash Deposits

Radiocarbon dating was performed on fifteen samples from cores collected at Saba Pond and Magens Bay in 2020 as well as samples from cores collected at Perseverance and Cabrita Ponds in 2014 to better constrain the ages of overwash deposits likely to be related to tsunamis. The results are presented in Table 5 along with previous dating results for samples from the 2014 cores. Radiocarbon ages for both sets of results were recalibrated using CALIB 8.2 (Stuiver et al., 2020) and the IntCal20 Northern Hemisphere radiocarbon age calibration curve (Reimer et al., 2020), except for Magens Bay sample 20-2A-1L-28-29 from core 2 collected in 2020 which was calibrated by Beta Analytic using BetaCal 3.21 high probability method (Bronks Ramsey, 2009) and IntCal13 (Reimer et al., 2013). The positions of the samples and the maximum and minimum values of the 2-sigma calibrated date ranges are shown on stratigraphic columns of the cores (Figures 10, 14, 17, 18, and 19) and on the event chronology (Figure 20).

Saba Pond

For Saba Pond, sample 20-4A-1P-61-63 collected above unit S-c yielded a 2-sigma calibrated date of A.D. 1152-1137 (4.7% probability), 1134-1081 (21.8% probability), and 1049-992 (73.5% probability), indicating that S-c was deposited before A.D. 1152 (Table 5; Figures 10 and 20). Sample 20-4A-1P-61-63 also indicates that the overlying unit S-d was deposited after A.D. 992. Samples 20-4A-1P-57 and 20-3A-1P-35 both from the sandy portion of S-d were similar in age to the underlying deposit suggesting that the two samples were reworked from the underlying unit. The basal contact of S-d is erosional and the underlying deposit completely removed in core 3, supporting the interpretation that samples 20-4A-1P-57 and 20-3A-1P-35 are from the underlying deposit and incorporated in S-d. Sample 20-4A-1P-44.3 collected immediately above unit S-d yielded a 2-sigma calibrated date of A.D. 1387-1362 (16.7% probability) and 1308-1263 (83.3% probability) indicating that S-d was deposited before A.D. 1387. The dates of the four samples collected above, below, and within unit S-d indicate that it was deposited between A.D. 1387 and A.D. 992. Unit S-d is interpreted to have been deposited during the A.D. 1480-1200 event. Dating at Saba Pond suggests the event occurred before A.D. 1390.

Sample 20-4A-1P-44.3 also provides a maximum constraining age of A.D. 1263 for unit S-e. Sample 20-4A-1P-28 collected with the lower part of S-e and sample 20-2A-1P-11 collected from the uppermost part of the unit yielded almost identical calibrated dates of A.D. 1950-1656 for 20-4A-1P-28 and A.D. 1950-1649 for sample 20-2A-1P-11. Given the depth of the unit S-e, the upper range of the calibrated dates can be excluded reducing the full range of the dates to A.D. 1880-1656 and A.D. 1878-1649. Given the similarity in their ages, the samples were likely from vegetation growing in or near the pond at the time of the event. The plant material of sample 20-4A-1P-28 was incorporated within the deposit; whereas the seeds of sample 20-2A-1P-11 may have settled out of suspension following the event. Unit S-e is interpreted to have formed during the A.D. 1800-1650 event, probably the 1755 Lisbon tsunami.

Sample 20-2A-1P-11 collected from the uppermost part of the unit S-e also provides a maximum constraining age of A.D. 1649 for unit S-f. Given the position of the unit about midway between unit S-e and the Hurricane Irma deposit, we hypothesize that S-f was deposited during the 1867 tsunami. We are testing this hypothesis with Pb-210 and Cs-137 dating of the upper portion of core 4. Results of the analyses are pending at the time of this writing.

Table 5. Radiocarbon dating results for St. Thomas study sites

Sample No. BA* Lab No.	Sample Material	Sample Context	Radiocarbon Age (Yr BP) [†]	Calibrated Calendar Years (AD/BC) [‡]	Probability Distribution (2-sigma) [#]
Saba					
20-2A-1P-11 Beta-562126	seed	core 2; uppermost part of S-e	190 ± 30	AD 1950-1916 1878-1871 1867-1851 1845-1837 1811-1725 1695-1649	0.186 0.009 0.015 0.010 0.550 0.230
20-4A-1P-28 Beta-562127	plant	core 4; within lower part of S-e	180 ± 30	AD 1950-1910 1880-1835 1813-1723 1697-1656	0.198 0.077 0.524 0.200
20-4A-1P-44.3 Beta-559776	plant	core 4; immediately above S-d	710 ± 30	AD 1387-1362 1308-1263	0.167 0.833
20-4A-1P-57 Beta-559775	plant	core 4; within S-d	990± 30	AD 1156-1078 1052-994	0.538 0.462
20-3A-1P-35 Beta-567844	plant	core 3; within S-d	1150 ± 30	AD 989-983 979-824 788-775	0.014 0.903 0.082
20-4A-1P-61-63 Beta-580442	plant	core 4; below S-d above S-c	1010±30	AD 1152-1137 1134-1081 1049-992	0.047 0.218 0.735
Magens Bay[¶]					
20-2A-1L-28-29	wood	core 2; within MB-e	60 ± 30	AD 1920-1811 1728-1692	0.724 0.230
Perseverance					
14-2A-1P-46 Beta-565220	plant	core 2; below P-f	70 ± 30	AD 1924-1810 1730-1690 [¶]	0.711 0.243
14-2A-1P-53-54 Beta-565221	plant	core 2; above P-e	140 ± 30	AD 1944-1903 1929-1800 1827-1798 1779-1770 1768-1671	0.180 0.316 0.115 0.022 0.367
14-2A-1P-86 Beta-567843	plant	core 2; between P-e and P-b	1470 ± 30	AD 646-559	1.0
14-3A-2B-35.5 Beta-389603	leaf	core 3; between P-e and P-b	1910 ± 30	AD 214-59 43-28	0.972 0.028
14-2A-2L-77 Beta-389602	leaf	core 2; above P-b	2380 ± 30	BC 393-542 655-660 710-716	0.977 0.012 0.011

Table 5 Continued. Radiocarbon dating results for St. Thomas study sites

Sample No. BA* Lab No.	Sample Material	Sample Context	Radiocarbon Age (Yr BP) [†]	Calibrated Calendar Years (AD/BC) [‡]	Probability Distribution (2-sigma) [#]
Perseverance					
14-3A-3L-40-40.2 Beta-565222	peat	core 3; below P-b	3180 ± 30	BC 1408-1505	1.0
14-3A-3L-77-77.2 Beta-576540	peat	core 3; above P-a	3190 ± 30	BC 1415-1506	1.0
Cabrita Pond					
14-3A-1P-72 Beta-565223*	wood	core 3; above C-d	400 ± 30	AD 1623-1575 1522-1438	0.223 0.777
CPN2-W1-33** Beta-325859	wood	above C-d	380 ± 30	AD 1632-1569 1567-1558 1525-1447	0.358 0.019 0.622
CPN2-W2-66** Beta-319295	twig	below C-d	1000 ± 30	AD 1153-1080 1050-993	0.408 0.592
14-1A-2B-8.5 Beta-389594	twig	core 1; below C-c above C-b	2160 ± 30	BC 57-71 97-232 247-256 280-355	0.022 0.588 0.010 0.380
14-2A-2B-30 Beta-389598	leaf	core 2; above C-c	1940 ± 30	AD 204-183 171-10	0.044 0.956
14-1A-2B-56.2 Beta-389595	leaf	core 1; below C-b	3280 ± 30	BC 1463-1473 1498-1619	0.021 0.979
14-1A-2B-74.5 Beta-389596	leaf	core 1; below C-b	3520 ± 30	BC 1749-1930	1.0
14-1A-2B-81.5 Beta-389597	leaf	core 1; above C-a	3580 ± 30	BC 1781-1790 1824-1841 1878-1987 1989-2027	0.013 0.036 0.808 0.143
14-2A-3B-98 Beta-389599	leaf	core 2; above C-a	3970 ± 30	BC 2349-2379 2404-2423 2441-2445 2447-2574	0.050 0.036 0.003 0.910
14-3A-5L-82-82.5 Beta-389600	charcoal or leaf	core 3; below C-a	4350 ± 30	BC 2899-3027 3064-3077	0.970 0.030
Smith Pond					
14-1B-1L-41-42 Beta-565226	wood	core 1; below S-e	660 ± 30	AD 1394-1353 1325-1279	0.492 0.508
14-1B-2L-22-22.2 Beta-576541	plant	core 1; above S-b	2040 ± 30	AD 61-37 AD 31-BC 118 132-150	0.044 0.927 0.029
14-1B-2L-62 Beta-389604	leaf	core 1; within S-b	2690 ± 30	BC 804-901	1.0
14-1B-2L-69-69.2 Beta-565227	plant	core 1; below S-b	2640 ± 30	BC 777-833 877-894	0.948 0.052

* Beta Analytic laboratory number.

** Organic samples published previously in Fuentes et al., 2017.

[†] Conventional radiocarbon age reported as radiocarbon years before present (BP), "present" = AD 1950, determined by Beta Analytic, Inc.

[‡] Calibrated calendar year ranges determined with Calib 8.2., Stuiver, M., Reimer, P.J., and Reimer, R.W., 2020, CALIB 8.2 [WWW program] at <http://calib.org>, accessed 2020-12-26.

[#] Reimer et al., 2020, The IntCal20 Northern Hemisphere radiocarbon age calibration curve (0-55 cal kB Radiocarbon 62. doi: 10.1017/RDC.2020.41.

[†] Calibrated calendar year ranges determined by Beta Analytic: BetaCal3.21 high-probability method (Bronk Ramsey, 2009) and IntCal13 (Reimer et al., 2013).

Magens Bay

For Magens Bay, sample 20-2A-1L-28-29 collected from the uppermost overwash deposit, MB-e, yielded a 2-sigma calibrated date of A.D. 1920-1811 (72.4% probability) and 1728-1692 (23.0% probability) (Table 5; Figures 14 and 20). The date range is quite broad spanning almost the entire historical period. If correlations of units MB-d and MB-e with the lower and upper overwash deposits in the 2012 Dutch spoon samples are correct, the dating of sample 20-2A-1L-28-29 supports the previous interpretation that the deposit is historical in age and could have resulted from the A.D. 1800-1650 event or 1755 Lisbon tsunami.

Perseverance Pond

For Perseverance Pond, sample 14-3A-3L-77-77.2 collected from peat above unit S-a yielded a 2-sigma calibrated date of B.C. 1415-1506 (100% probability), indicating that S-a was deposited before B.C. 1415 (Table 5; Figures 17 and 20). Sample 14-3A-3L-40-40.2 collected from the same peat but below unit P-b was very similar in age to sample 14-3A-3L-77-77.2 and indicated that P-b was deposited after B.C. 1505. Sample 14-2A-2L-77 collected above P-b yielded a calibrated date of B.C. 393-542 (97.7% probability), 655-660 (1.2% probability), 710-716 (1.1% probability) providing a minimum constraining date of B.C. 393 for P-b (Figure 17). The dates of the two samples collected above and below unit P-b indicate that it was deposited between B.C. 393 and B.C. 1505.

Sample 14-2A-1P-86 collected from a sandy mud below unit P-e yielded a calibrated date of A.D. 646-559 indicating that the overlying unit was deposited after A.D. 559. Sample 14-2A-1P-53-54 collected immediately above unit P-e provided a calibrated date of A.D. 1944-1903 (18.0% probability), 1929-1800 (31.6% probability), 1827-1798 (11.5% probability), 1779-1770 (2.2% probability), and 1768-1671 (36.7% probability). Sample 14-2A-1P-46, collected 8 cm higher in the section and below unit P-f, was very similar in age with a calibrated date of A.D. 1924-1810 (71.1% probability) and 1730-1690 (24.3% probability). The dates of the samples collected above and below unit P-e indicate that it was deposited between A.D. 559 and A.D. 1944 and the date of the sample collected below P-f indicate that it was deposited after A.D. 1690. Given the dating results and relative positions of the two overwash deposits in the upper 80 centimeters of the cores, we hypothesize that the lower unit P-e was deposited during the A.D. 1800-1650 event, or 1755 Lisbon tsunami, and the upper unit P-f was deposited during the 1867 tsunami known to have inundated the southern coast in nearby Charlotte Amalie. We are testing these hypotheses with Pb-210 and Cs-137 dating of the upper portion of core 2. Results of the analyses are pending.

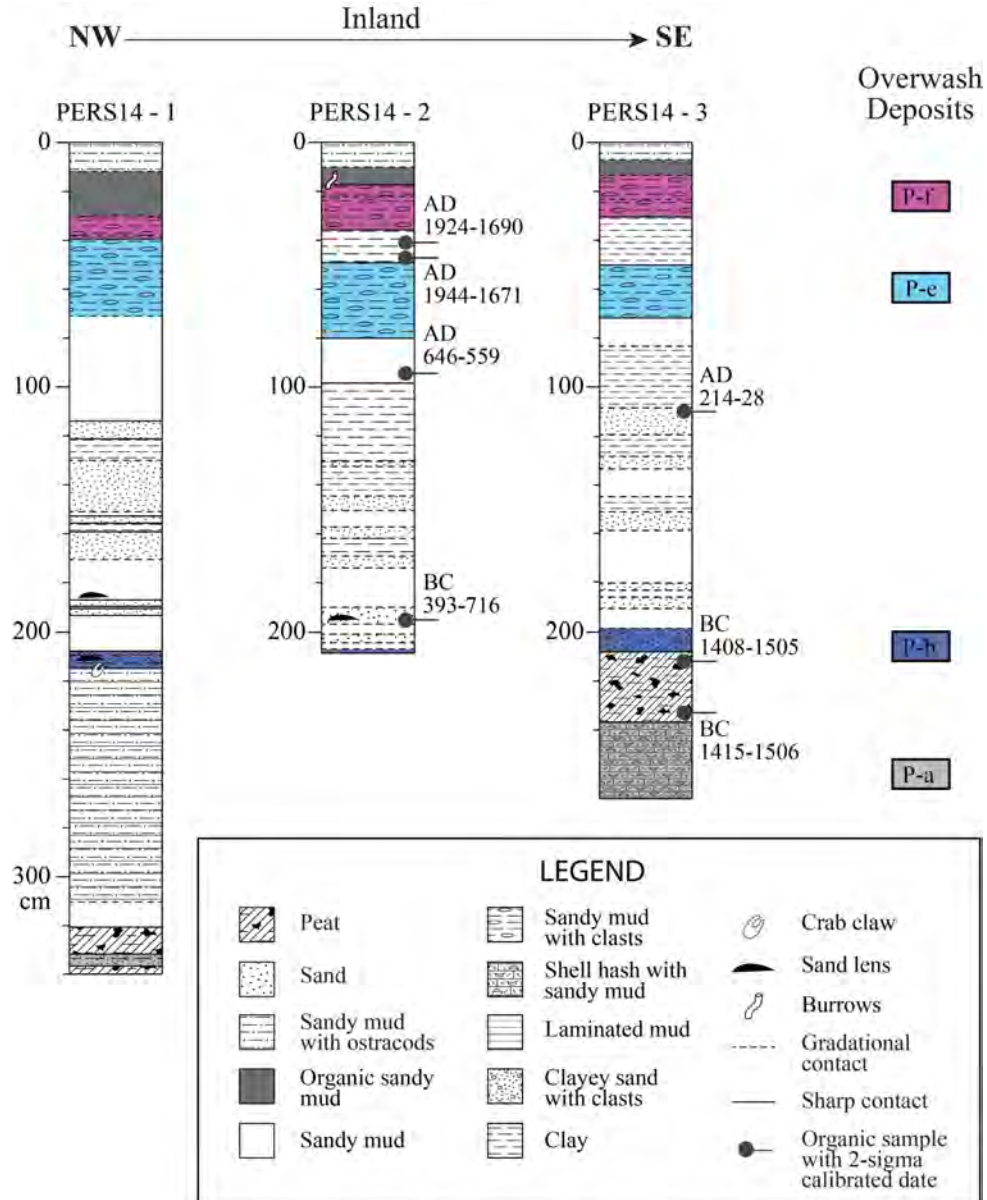


Figure 17. Stratigraphic columns based on interpretation of sediment cores collected at Perseverance Pond in 2014 (see Appendix for photographs of cores). Hurricane Irma overwash deposit (S-g), clearly captured in core 1, thinned abruptly between core 1 and 2 and appears to have extended across most of the pond to core 4. Overwash deposits S-c, S-d, S-e, and S-f are interpreted as likely tsunami deposits.

Cabrita Pond

For Cabrita Pond, samples 14-3A-5L-82-82.5 and 14-2A-3B-98 provide maximum and minimum constraining ages of B.C. 3077 and B.C. 2349, respectively, for unit C-a (Table 5; Figures 18 and 20). Sample 14-1A-2B-56.2 and 14-1A-2B-8.5 provide maximum and minimum constraining ages of B.C. 1619 and B.C. 57, respectively, for unit C-b. Sample 14-1A-2B-8.5 also provides a maximum constraining age of B.C. 355 for Unit C-c. Sample 14-2A-2B-30 collected immediately above C-c yielded a calibrated date of A.D. 204-183 (4.4% probability) and A.D. 171-10 (95.6% probability), providing a close minimum age of A.D. 204. Therefore,

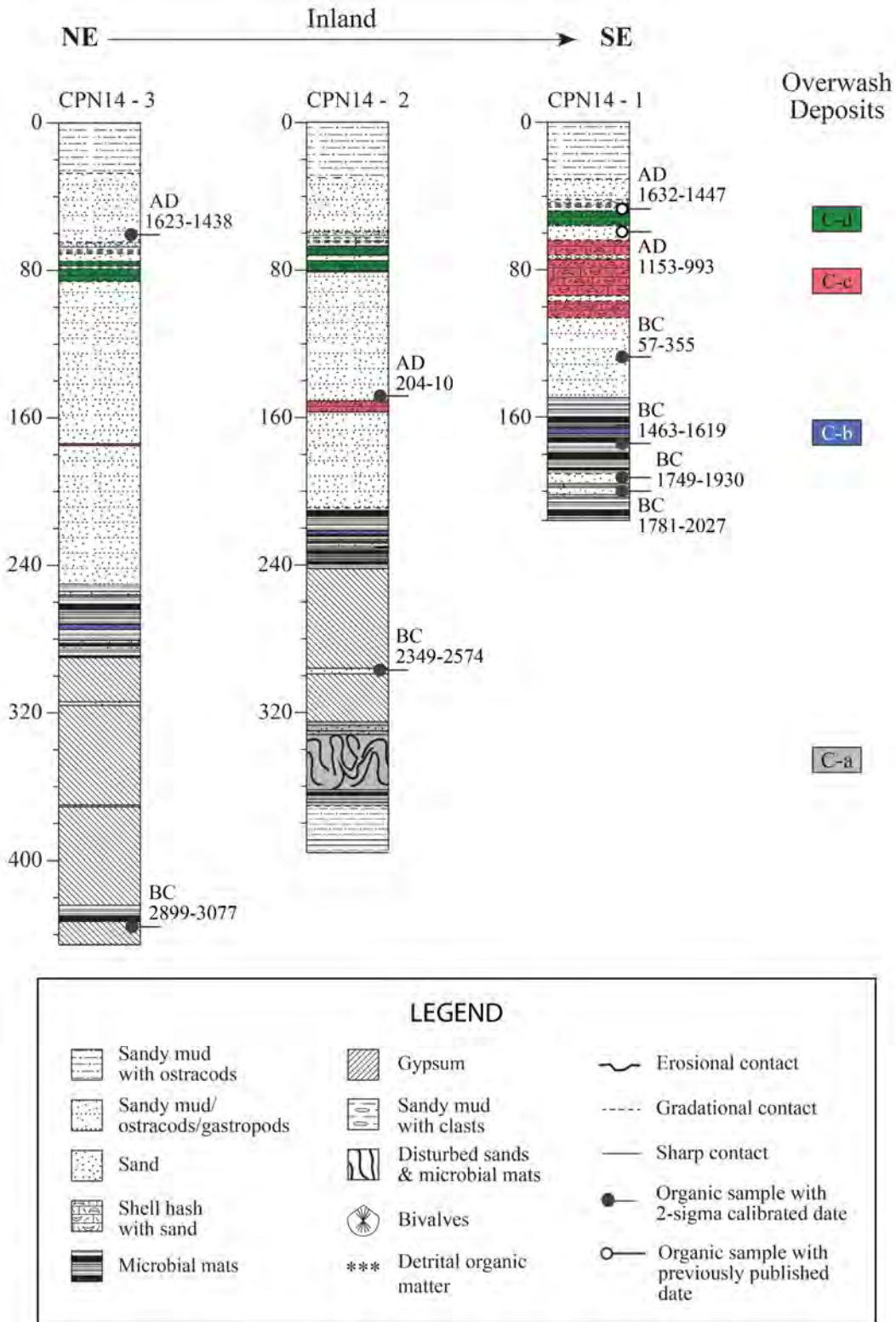


Figure 18. Stratigraphic columns based on interpretation of sediment cores collected at Cabrita Pond in 2014 (see Appendix for photographs of cores). Storm surge from Hurricane Irma was not great enough to produce an overwash deposit recorded in the pond sedimentary record. Overwash deposits S-c, S-d, S-e, and S-f are interpreted as likely tsunami deposits.

unit C-c was deposited between A.D. 204 and B.C. 355 and more likely during the younger end of the period (Table 5; Figures 18). Sample CPN2-W2-66 with a calibrated date of A.D. 1153-1080 (40.8% probability) and 1050-993 (59.2% probability) provides a maximum constraining age of A.D. 993 for unit C-d. Samples 14-3A-1P-72 and CPN2-W1-33 both collected above C-d yielded similar results with ranges of A.D. 1623-1438 and A.D. 1632-1447 that provide maximum constraining ages of A.D. 1623 and A.D. 1632, respectively (Table 5). From dating of samples above and below Unit C-d, the overwash deposit formed between A.D. 1623 and A.D. 993. Although it is not required, it is likely that C-d was deposited during the A.D. 1480-1200 event.

Smith Pond

No new radiocarbon dating was performed for samples from Smith Pond cores collected in 2014 but the previous dating results were recalibrated for this study (Table 5; Figures 19 and 20). Descriptions of the cores and likely tsunami deposits can be found in Fuentes et al. (2019).

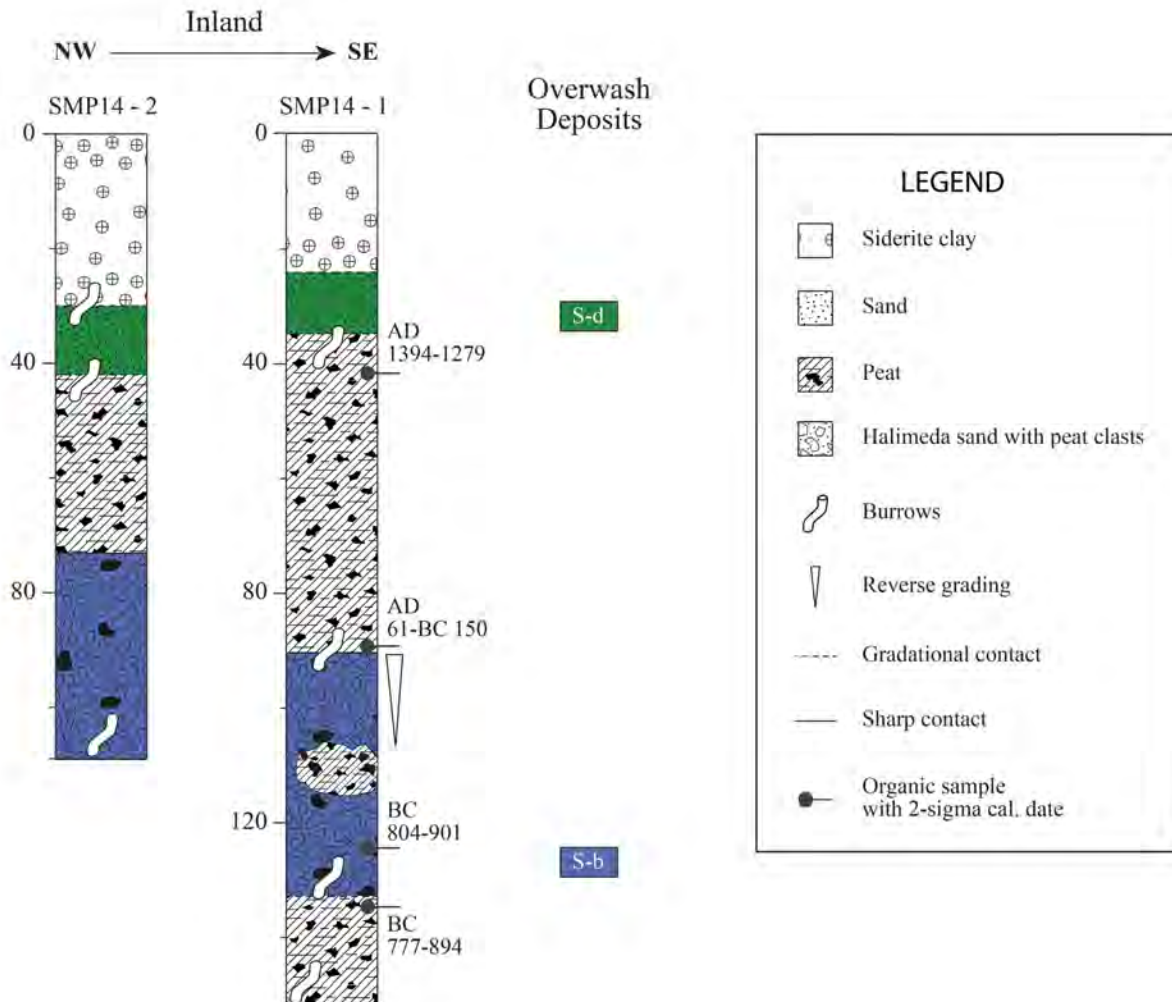


Figure 19. Stratigraphic columns based on interpretation of sediment cores collected at Smith Pond in 2014 (see Fuentes et al., 2017). SMP14-1 is a compilation of 1a and 1b. Overwash deposits S-b and S-d are interpreted as likely tsunami deposits that were deposited circa B.C.390-890 and A.D. 1480-1200.

Samples 14-1B-2L-69-69.2 and 14-1B-2L-22-22.2 collected from peat below and above unit S-b provide maximum and minimum constraining ages for the Halimeda sand with peat clasts of B.C. 894 and A.D. 61, respectively. Sample 14-1B-2L-62, a leaf from the unit S-b itself, provides a close maximum date of B.C 804-901 (100% probability). The three samples taken together suggest that S-b was deposited between A.D 61 and B.C 894 and probably towards the older end of the period. Sample 14-1B-1L-41-42 from peat provides a maximum constraining age of A.D. 1270 for the overlying unit S-d. There are no minimum constraining dates for unit S-d. Given the depth of the deposit and the maximum constraining date, it is likely that S-d was deposited during the A.D. 1480-1200 event.

2017 HURRICANE IRMA AND 1867 TSUNAMI DEPOSITS ON ST. THOMAS

Hurricane Irma Deposits

Hurricane Irma provided an opportunity to characterize storm deposits at our study sites and to revisit criteria used to distinguish likely tsunami deposits from storm deposits in the pond sediments. Although their barrier bars are of similar height, ~2 m above MHHW, category 5 Hurricane Irma and its storm surge only formed overwash deposits in Saba Pond and along a stream at Magens Bay. Both sites have northwestern aspects and would have been vulnerable to waves driven by winds out of the northwest (Table 6). In contrast, storm surge was not great enough to transport sediment over the barrier bars and into Perseverance, Smith, and Cabrita Ponds. Perseverance Pond, on the southern side of the island and with a southern aspect, was likely protected from the worst of the storm surge. Smith Pond is more than 100 m from the shoreline, and Cabrita Pond's barrier bar is armored with pebbles, cobbles, and boulders.

At Saba Pond, Hurricane Irma's storm surge produced overwash fans that built into the pond and an overwash deposit appears to extend up to 80 m across the bottom of the pond (Table 6). Closer to the barrier bar, the overwash deposit is ~4 cm thick and composed of very well sorted and coarsening upward, medium to coarse carbonate sand with a few lithics and shell fragments. The deposit quickly thins inland to ~1 cm and becomes a moderately well sorted, fine to medium carbonate sand. At Magens Bay, Hurricane Irma's storm surge produced a broadly distributed overwash deposit that extended ~60 m inland and even farther ~250 m along a stream. As documented at a site along the stream and near a ponded area where overwash deposits were observed in Dutch spoon samples in 2012, Hurricane Irma's overwash deposit was ~1 cm thick and composed of moderately well sorted, medium carbonate sand with a small amount of clayey silt, foraminifera, diatoms, and siliceous biogenic components. In the floodplain setting, the deposit probably will be destroyed over time by crab and mangrove root bioturbation. The deposit is more likely to be preserved as a thin carbonate sand layer in the nearby ponded area.

Hurricane Irma deposits are similar to other documented storm deposits in that they formed immediately behind barrier bars and extend into ponds and along streams; they thin and fine inland; they are well to moderately well sorted and are composed primarily of reworked sediment from the foreshore and backshore zones; and their geographical distribution can be related to the track of the storm (Tables 1 and 6). For Hurricane Irma, overwash deposits formed at sites with northwest exposures that would have been subject to storm surge driven by northwest winds as the hurricane past to the north of St. Thomas.

Table 6. Characteristics of 2017 Hurricane Irma and 1867 Tsunami deposits

Characteristic	2017 Hurricane Irma	1867 Tsunami
Composition	At Magens Bay and Saba Pond, mostly carbonate sand	At Saba Pond, mostly carbonates; at Perseverance Pond, mostly carbonate sand but also includes small amount of sand, silt, and clay
Biota	At Magens Bay, foraminifera and diatoms; at Saba Pond, some marine bivalve shells	At Saba Pond, ostracod shell fragments, fine-sand size foraminifera and organics; at Perseverance Pond, <i>Halimeda</i> segments and organics
Sorting	Well sorted at Saba Pond; moderately sorted at Magens Bay	Somewhat poorly sorted at Saba Pond; poorly sorted at Perseverance Pond
Grading	Reverse grading at Saba	Normal grading at Saba
Sedimentary structures	At Magens Bay discontinuous layers; at Saba Pond, massive to weakly bedded	At Saba Pond, two parallel beds; at Perseverance Pond, massive
Rip-up clasts	Not present	at Saba Pond, not present; at Perseverance Pond, clasts of green clay from underlying deposit
Bed thickness	At Magens Bay, up to 2 mm thick; at Saba Pond, up to 5 cm thick near barrier bar, abruptly thins inland to <1 cm	At both Saba and Perseverance, ranges up to 20 cm thick, maintains thickness (+/- 5 cm) across pond
Contacts	At Saba, sharp basal contact	At Saba and Perseverance Ponds, sharp basal contact
Morphology	At Magens Bay, overwash fans occur inland of barrier bar, across coastal plain, and along stream floodplain; at Saba, overwash deposit extends into pond and thins inland	Sheet deposit at both Perseverance and Saba Ponds
Inland extent (limited by steep topography)	At Magens Bay, up to 250 m along stream; at Saba, up to 80 m into pond	At both Saba and Perseverance Ponds, at least 100 m across the ponds
Areal distribution	Both northern and southern coasts; Magens Bay and Saba Pond with northwestern aspects	Southern coast, Saba and Perseverance Ponds in direct path of tsunami

1867 Tsunami Deposits

The 1867 tsunami originating in Anegada Passage is known to have inundated numerous islands across the Caribbean, including St. Thomas where it reached wave heights of 6 m at Charlotte Amalie and 12 m at Water Island off the southern coast of the St. Thomas. Therefore, the tsunami is likely to have inundated coastal sites on the southern side of St. Thomas, where we found likely candidates for 1867 tsunami deposits in cores collected in Saba and Perseverance Ponds in 2020 and 2014, respectively. The stratigraphic positions of the deposits and radiocarbon dates of samples collected below the deposits support the interpretation that they are related to the 1867 tsunami. This interpretation is being tested with Pb-210 and Cs-137 dating of the core sediment but the dating results are still pending.

At Saba Pond, unit S-f thought to be related to the 1867 tsunami, is 4-5 cm thick across the pond, has a sharp basal contact, fines upward and inland, and is composed of somewhat poorly sorted, very coarse to very fine carbonate sand with heavy minerals, lithic grains, ostracod shell fragments, foraminifera, and organics (Figure 20). At Perseverance Pond, unit P-f also thought to be related to the tsunami, varies from 8-18 cm thick across the pond, has a sharp basal contact, is composed of poorly sorted, carbonate sand with some silt and clay, clasts of the underlying green clay, *Halimeda* segments, and organics.

The deposits thought to be related to the 1867 tsunami exhibited many of the characteristics of documented tsunami deposits. They are sheet deposits with sharp basal contacts, that maintain thickness as they extend across ponds; they are poorly sorted, normally graded, and composed of a mixture of carbonate sand, lithic grains, broken shell fragments, and clasts of underlying deposits. For the 1867 tsunami, overwash deposits were only found at pond sites on the southern side of St. Thomas in the pathway of the tsunami propagating from the Anegada Passage.

EVENT CHRONOLOGY

The overwash deposits a, b, c, d, e described above in the sections on Site Investigations and Dating of Overwash Deposits are interpreted as likely tsunami deposits on the basis of their characteristics and differences with storm deposits (Table 6) and ages relative to historical tsunamis and to other likely tsunami deposits identified on Anegada (Figure 20). Previously, the following characteristics were used to interpret overwash deposits as likely tsunami deposits in pond sediment on St. Thomas: mixed composition of sediment derived from multiple environments of deposition, presence of broken shells, rip-up clasts, and mixed or disturbed sediment, and coincidence with changes to the environment of deposition. With the benefit of comparing overwash deposits related to 2017 Hurricane Irma with those thought to be related to the 1867 tsunami, characteristics of likely tsunami deposits are expanded to include sharp, sometimes erosional, basal contacts, one or more fining upward layers of mixed sediment or disturbed sediment including carbonate grains, lithics, shells, and rip-up clasts, that span most if not the entire width of the ponds (Table 6). Other thin, often discontinuous, overwash deposits that do not exhibit these characteristics are probably related to storms.

The 1867 tsunami (f) originating in the Anegada Passage south of St. Thomas appears to have left its mark at Saba and Perseverance Ponds on the southern side of St. Thomas (Figure 20). The A.D. 1800-1650 event (e), also observed on Anegada, probably was the A.D. 1755

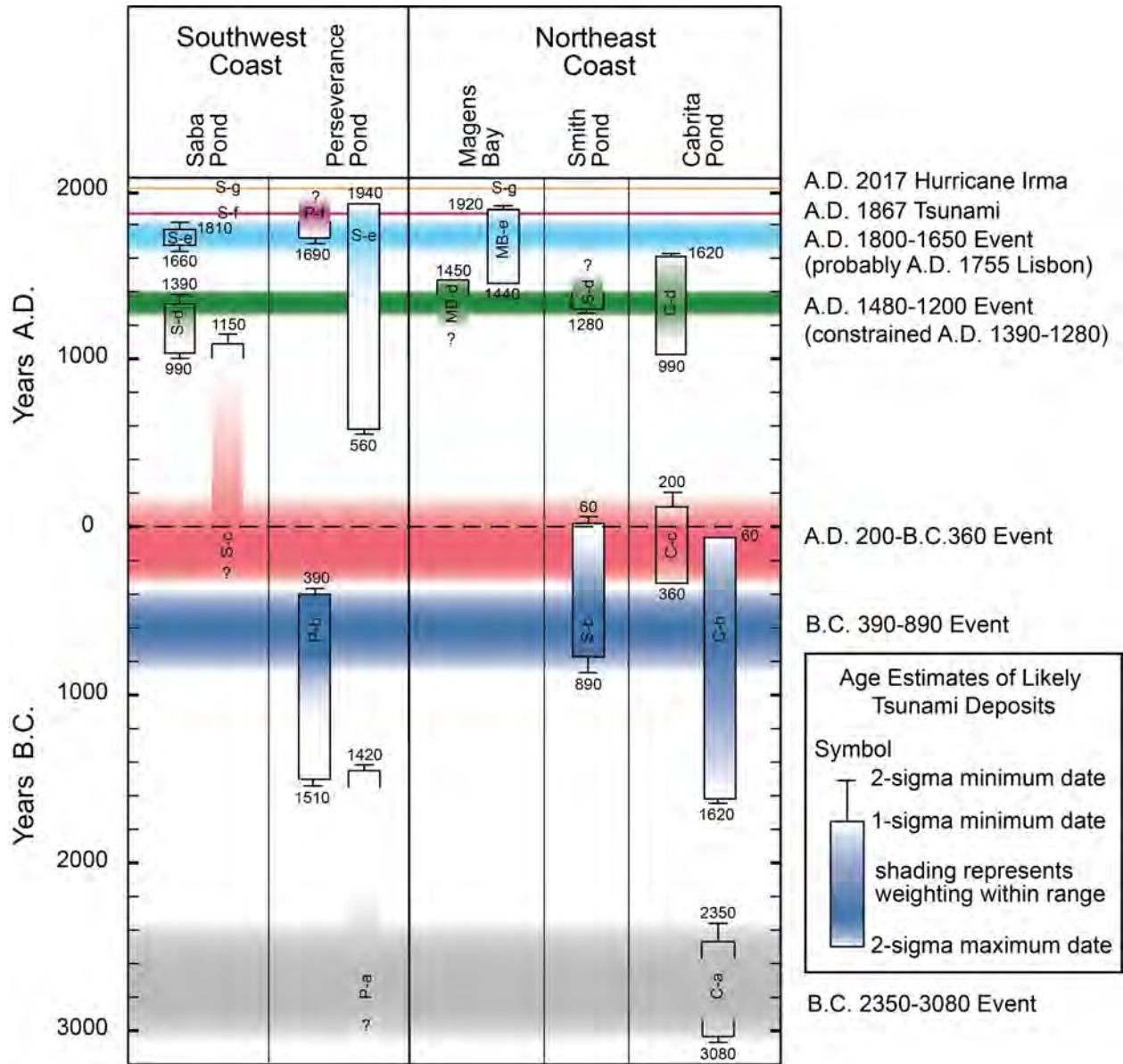


Figure 20. Event chronology showing dating results and age estimates of overwash deposits at study sites on the southwestern and northeastern coasts of St. Thomas.

Lisbon tsunami known to have inundated other islands in the northeastern Caribbean. This event appears to have produced overwash deposits at Saba and Perseverance Ponds and at Magens Bay on the northern coast of St. Thomas. The A.D. 1480-1200 event (d), first recognized on Anegada and likely caused by a $M > 8$ earthquake generated by the Puerto Rico subduction zone or related faults north of the BVI, is recorded at Magens Bay and Cabrita and Smith Ponds on the northeastern coast of the island as well as Saba Pond to the south. Dating during this study suggest that timing of the event can be narrowed to A.D. 1390-1280. The A.D. 200-B.C. 360 event (c) affected Cabrita Pond and possibly Saba Pond. The interpretation of this event at Saba is very tenuous given poor age control. Therefore, the event is only observed with certainty at Cabrita, suggesting that the tsunami may be very localized perhaps due to offshore slumping. The B.C. 390-890 event (b) was recorded at ponds on the northern and southern coasts including

Cabrita, Smith, and Perseverance Ponds. At the other two sites, Saba Pond and Magens Bay, the cores did not extend deep enough to determine if a related deposit does or does not occur at the sites. Given the distribution of the related deposits on both coasts, the B.C. 390-890 event appears to have been as significant tsunami as the A.D. 1480-1200 event but may have had a different source. Both the A.D. 1480-1200 and B.C. 390-890 event, and none of the other events, are recorded at Smith Pond which is the farthest (~140 m) pond from the shore. This too suggests that the A.D. 1480-1200 and the B.C. 390-890 events were similar in relative magnitude and more severe in their impacts on St. Thomas than the other likely tsunamis. The B.C. 2350-3080 event (a) affected Cabrita Pond and possibly Perseverance Pond, but the interpretation of this event at Perseverance is also tenuous due to poor age control. The strongest evidence for this event is at Cabrita Pond, but the record is limited at the other three sites by the depth of coring. Deeper coring at these sites may uncover additional evidence for this event.

CONCLUSION

In 2017, category 5 Hurricane Irma with winds speeds of 184 mph and gusts of 224 mph passed ~25 km north of St. Thomas. Wind-driven storm surge exceeded the height (~2 m) of barrier bars and lead to the formation of overwash deposits at five study sites on the northeastern coast, southwestern coast, and on Saba Islet off the southern coast of St. Thomas. Only at Saba Pond, did the overwash deposit extend into the coastal pond. At Magens Bay, overwash deposits formed across the backshore area and the floodplain along a stream. Both Saba Pond and Magens Bay have northwestern aspects that may have made them more vulnerable to storm surge from Hurricane Irma. In cores collected in Saba Pond and on the floodplain adjacent to the stream at Magens Bay, the overwash deposits are 1-4 cm thick, fairly well sorted, and composed primarily of carbonate sand. In Saba Pond, the deposit thinned and fined inland.

In 1867, a tsunami originating in Anegada Passage inundated numerous islands across the Caribbean, including St. Thomas where it reached wave heights of 6 m at Charlotte Amalie. We found overwash deposits that are likely related to the 1867 tsunami in cores collected at Saba Pond in 2020 and at Perseverance Pond in 2014. They are sheet deposits with sharp contacts, composed of somewhat poorly sorted, normally graded, carbonate sand with lithic grains, broken shell fragments, and clasts of underlying deposits.

On the basis of information gained about overwash deposits produced by Hurricane Irma and the 1867 tsunami, as well as other storms and tsunamis, three, possibly five, major overwash events are interpreted as likely tsunamis. In addition to the 1867 tsunami, these events include (1) the A.D. 1800-1650 event also observed on Anegada, BVI, and probably the A.D. 1755 Lisbon tsunami known to have inundated other islands in the northeastern Caribbean, (2) the A.D. 1480-1200 event first recognized on Anegada and likely caused by a $M > 8$ earthquake generated by the Puerto Rico subduction zone or related faults north of the BVI, (3) an event in B.C. 390-890 that appears to have been as significant as the A.D. 1480-1200 event, and two less certain events in A.D. 200-B.C. 360 and B.C. 2350-3080. With additional study and deeper coring at several of the sites it may be possible to gain more information about the events. Nevertheless, the sediment record in coastal ponds at St. Thomas suggests that there were at least two very large offshore earthquakes during the past ~3000 years.

ACKNOWLEDGMENTS AND DISCLAIMER

Martitia Tuttle and Zamara reviewed pre- and post-Irma imagery to identify overwash deposits and other effects of storm surge. Fuentes Zamara Fuentes, Carlos Vélez, Wilford Schmidt, and Laurel Bauer performed reconnaissance for and documentation of storm surge effects and collection of sediment cores at Saba and Cabrita Ponds and Magens Bay. Roy Watlington, Emeritus, University of the Virgin Islands, shared his knowledge of history of St. Thomas and seismic and tsunami hazards of the region and facilitated our fieldwork on the island. Paul Jobsis of the Center for Marine and Environmental Studies at the University of the Virgin Islands arranged boat transportation to Saba Islet. We are grateful to the government official and agencies as well as property owners who permitted work at the study sites, including Hubert Brumant of the Magens Bay Authority, Dr. Sean Kelly, Dr. Nicole F. Angeli and Alfonso García of the USVI Division of Fish and Wildlife, Department of Planning and Natural Resources, and Sean L. Krigger of VI State Historic Preservation Office. Zamara Fuentes and LacCore staff conducted descriptions, sampling, and analysis of the cores at LacCore at the University of Minnesota. Fuentes's work at the laboratory was cut short when the University of Minnesota and LacCore shut down in March 2020 due to Covid-19. We are grateful to Jessica Heck and other LacCore staff members who helped to complete core sampling and analysis when the laboratory reopened to staff members only. Beta Analytic, Inc. performed radiocarbon dating of organic samples collected from the cores. Amy Corp and Teledyne performed Pb-210 and Cs-137 analysis and interpretation. Because of delays related to the coronavirus pandemic, the interpretation of the results has not yet been completed. The results will be incorporated into a forthcoming article for publication. The material presented in this report is based upon work supported by the National Earthquake Hazard Reduction Program and the U.S. Geological Survey under Grant No. G19AP00101. The views and conclusions contained in this document are those of the authors and should not be interpreted as representing the opinions or policies of the U.S. Geological Survey. Mention of trade names or commercial products does not constitute their endorsement by the U.S. Geological Survey.

REFERENCES

- Atlantic and Gulf of Mexico Tsunami Hazard Assessment Group (2008). Evaluation of Tsunami Sources with the Potential to Impact the U.S. Atlantic and Gulf Coasts - A report to the Nuclear Regulatory Commission: U.S. Geological Survey Administrative Report, 322.
- Atwater, B. F., S. Musumi-Rokkaku, K. Satake, Y. Tsuji, K. Ueda, and D. K. Yamaguchi (2005). The orphan tsunami of 1700; Japanese clues to a parent earthquake in North America, U.S. Geological Survey Professional Paper 1707, 133 p. (published jointly by University of Washington Press, Seattle).
- Atwater, B. F., U. S. ten Brink, M. Buckley, R. S. Halley, B. E. Jaffe, A. M. López-Venegas, E. G. Reinhardt, M. P. Tuttle, S. Watt, and Y. Wei (2012). Geomorphic and stratigraphic evidence for an unusual tsunami or storm a few centuries ago at Anegada, British Virgin Islands, *Nat. Hazards* **63**, no. 1, 51-84.
- Atwater, B. F., Z. Fuentes, R. B. Halley, U. S. Ten Brink, and M. P. Tuttle (2014). Effects of 2010 Hurricane Earl amidst geologic evidence for greater overwash at Anegada, British Virgin Islands, *Advances in Geosciences* **38**, 21-30.

- Atwater, B. F., U. S. ten Brink, A. L. Cescon, N. Feuillet, Z. Fuentes, R. B. Halley, C. Nuñez, E. G. Reinhardt, J. H. Roger, Y. Sawai, M. Spiske, M. P. Tuttle, Y. Wei, Y., and J. Weil-Accardo, (2017). Extreme waves in the British Virgin Islands during the last centuries before 1500 CE, *Geosphere* **13**, no. 2, 301-368.
- Bilek, S. L., and T. Lay (2018). Subduction zone megathrust earthquakes, *Geosphere* **14**, no. 4, 1468-1500.
- Bronk Ramsey, C. (2009). Bayesian analysis of radiocarbon dates, *Radiocarbon* **51**, no.1, 337-360.
- Flores, C. H., U. ten Brink, W. H. Bakun (2012). Accounts of damage from historical earthquakes in the northeastern Caribbean, to aid in the determination of their location and intensity magnitudes, U.S. Geological Survey Open-File Report 2011-1133, 199 p.
- Fuentes, Z., M. P. Tuttle, and W. E. Schmidt (2017). Sand scripts of past tsunamis in coastal ponds of St. Thomas, U.S. Virgin Islands, *Seismol. Res. Lett.* **88**, no. 6, 1516-1526.
- Fukushima, Y., 2015, The contribution of palaeoseismology to seismic hazard assessment in site evaluation for nuclear installations, Y. Fukushima (Editor), International Atomic Energy Agency, Vienna, Austria, 1-193.
- Goff, J., B. G. McFadgen, J. Goff, B. G. McFadgen, and C. Chague-Goff (2004). Sedimentary differences between the 2002 Easter storm and the 15th-century Okoropunga tsunami, southeastern North Island, New Zealand, *Marine Geology* **204**, no. 1-2, 235-250.
- Goto, K., C. Chagué-Goff, S. Fujino, J. Goff, B. Jaffe, Y. Nishimura, B. Richmond, D. Sugawara, W. Szczuciński, D. R. Tappin, R. C. Witter, and E. Yulianto (2011). New insights of tsunami hazard from the 2011 Tohoku-oki event, *Marine Geology* **290**, 46-50.
- Goto, T., K. Satake, T. Sugai, T. Ishibe, T. Harada, and S. Murotani (2015). Historical tsunami and storm deposits during the last five centuries on the Sanriku coast, Japan, *Mar. Geol.* **367**, 105-117.
- Hüpers, A., M. E. Torres, S. Owari, L. C. McNeill, B. Dugan, T. J. Henstock, K. L. Milliken, K. E. Petronotis, J. Backman, S. Bourlange, *et al.* (2017). Release of mineral-bound water prior to subduction tied to shallow seismogenic slip off Sumatra, *Science* **356**, no. 6340, 841-844.
- Jamison-Todd, S., Stein, N., Overeem, I., Khalid, A., and Trower, E. J. (2020). Hurricane deposits on carbonate platforms: A case study of Hurricane Irma deposits on Little Ambergris Cay, Turks and Caicos Islands, *JGR: Earth Surface*, **124**, 1-16.
- Kelsey, H. M., A. R. Nelson, E. Hemphill-Haley, and R. C. Witter (2005). Tsunami history of an Oregon coastal lake reveals a 4600 yr record of great earthquakes on the Cascadia subduction zone, *Geological Society of America Bulletin*, **117**, 1009-1032.
- Kennedy, A. B., N. Mori, Y. Zhang, T. Yasuda, S.-E. Chen, Y. Tajima, W. Pecor, and K. Toride (2016). Observations and modeling of coastal boulder transport and loading during super typhoon Haiyan, *Coastal Engineering Journal* **58**, 1-25.
- Kortekaas, S. and A.G. Dawson (2007). Distinguishing tsunami and storm deposits: An example from Martinhal, SW Portugal, *Sedimentary Geology* **200**, 208-221.
- López, A. M., S. Stein, T. H. Dixon, G. Sella, E. Calais, P. Jansma, J. C. Weber, and P. LaFemina (2006). Is there a northern Lesser Antilles forearc block?, *Geophys. Res. Lett.* **33**, no. 7, 1-4.
- McCann, W. R. (1985). On the earthquake hazards of Puerto Rico and the Virgin Islands, of *Bulletin of the Seismological Society of America* **75**, 251-262.

- Minoura, K., F. Imamura, D. Sugawara, Y. Kono, and T. Iwashita (2001). The 869 Jogan tsunami deposit and recurrence interval of large-scale tsunami on the Pacific coast of northeast, Japan, *Journal of Natural Disaster Science* **23**, 83-88.
- Mueller, C. S., A. D. Frankel, M. D. Petersen, and E. V. Leyendecker (2003). Documentation for 2003 USGS seismic hazard maps of Puerto Rico and the U.S. Virgin Islands, U.S. Geological Survey, Golden, Colorado, Open file report 03-379.
- Morton, R. A., J. R. Goff, and S. L. Nichol (2008). Hydrodynamic implications of textural trends in sand deposits of the 2004 tsunami in Sri Lanka, *Sediment Geol* **207**, no. 1-4, 56-64.
- Nanayama, F., K. Shigeno, K. Satake, K. Shimokawa, K. Koitabashi, S. Miyasaka, and M. Ishii (2000). Sedimentary differences between the 1993 Hokkaido-nansei-oki tsunami and the 1959 Miyakojima typhoon at Taisei, southwestern Hokkaido, northern Japan, *Sedimentary Geology* **135**, 255-264.
- Namegaya, Y., K. Sataki, and S. Yamaki (2010). Numerical simulation of the 869 Jogan tsunami in Ishinomaki and Sendai plains and Ukedo river-mouth lowland, 活断層・古地震研究報告, n. 10, 9-29.
- National Geodetic Survey (2021) (2017). NOAA NGS Emergency Response Imagery: Hurricane Irma, <https://www.fisheries.noaa.gov/inport/item/52284>.
- Nelson, A. R., H. M. Kelsey, and R. C. Witter (2006). Great earthquakes of variable magnitude at the Cascadia subduction zone, *Quaternary Research* **65**, 354-365.
- Nelson, A. R., R. W. Briggs, T. Dura, S. E. Engelhart, G. Gelfenbaum, L.-A. Bradley, S. L. Forman, C. H. Vane, and K. A. Kelley (2015). Tsunami recurrence in the eastern Alaska-Aleutian arc: A Holocene stratigraphic record from Chirikof Island, Alaska, *Geosphere* **11**, 1-34.
- O'Loughlin, K. F., and J. F. Lander (2003). Caribbean Tsunamis-A 500-Year History from 1498-1998, Kluwer Academic Publishers, The Netherlands.
- Peters, R., and B. E. Jaffe (2010). Identification of tsunami deposits in the geologic record; developing criteria using recent tsunami deposits, U. S. Geological Survey Open-File Report 2010-1239, 39 p. [<http://pubs.usgs.gov/of/2010/1239/>].
- Pilarczyk, J. E., B. P. Horton, J. L. A. Soria, A. D. Switzer, F. Siringan, H. M. Fritz, N. S. Khan, S. Ildelfonso, A. A. Doctor, and M. L. Garcia (2016). Micropaleontology of the 2013 Typhoon Haiyan overwash sediments from the Leyte Gulf, Philippines: *Sedimentary Geology* **339**, 104-114.
- Pilarczyk, J., Spiske, M., Stephen, M. (2021). Distinguishing between hurricane and tsunami deposition using modern analogues from Anegada, British Virgin Islands (BVI), *EGU General Assembly Conference Abstracts*, **EGU21-10233**.
- Reicherter, K., D. Vonberg, B. Koster, T. Fernández-Steeger, C. Grützner, and M. Mathes-Schmidt (2010). The sedimentary inventory of tsunamis along the southern Gulf of Cádiz (SW Spain), *Zeitschrift für Geomorphologie (Supplementary Issue)* **54**, n. 3, 147-173.
- Reid, H., and S. Taber (1919). The Puerto Rico earthquakes of October-November 1918, *Bulletin of the Seismological Society of America* **9**, 95-127.
- Reinhardt, E., J. Pilarczyk, and A. Brown (2012). Probable tsunami origin for a shell and sand sheet from marine ponds on Anegada, British Virgin Islands: *Natural Hazards* **63**, 101-117, doi:10.1007/s11069-011-9730-y.
- Reimer, P. J., E. Bard, A. Bayliss, J. W. Beck, P. G. Blackwell, C. Bronk Ramsey, P. M. Grootes, T. P. Guilderson, H. Hafliðason, I. Hajdas, C. HattĹ, T. J. Heaton, D. L. Hoffmann, A. G. Hogg, K. A. Hughen, K. F. Kaiser, B. Kromer, S. W. Manning, M. Niu,

- R. W. Reimer, D. A. Richards, E. M. Scott, J. R. Southon, R. A. Staff, C. S. M. Turney, and J. van der Plicht, (2013). IntCal13 and Marine13 radiocarbon age calibration curves 0-50,000 years cal BP, *Radiocarbon* **55**, no. 4, 1869-1887.
- Reimer P. J., W. E. N. Austin, E. Bard, A. Bayliss, et al. (2020). The IntCal20 Northern Hemisphere radiocarbon age calibration curve (0-55 cal kB, *Radiocarbon* **62**. doi: 10.1017/RDC.2020.41.
- Rhodes, B., M. Tuttle, B. Horton, L. Doner, H. Kelsey, A. Nelson, M. Cisternas (2006). Paleotsunami research, American Geophysical Union, EOS, v. 87, n. 21, p. 205, 209.
- Schnurrenberger, D., J. Russell, and K. Kelts (2003). Classification of lacustrine sediments based on sedimentary components, *J Paleolimnol* **29**, 141-154.
- Soria, J. L. A., A. D. Switzer, C. L. Villanoy, H. M. Fritz, P. H. T. Bilgera, O. C. Cabrera, F. P. Siringan, Y. Y.-S. Maria, R. D. Ramos, and I. Q. Fernandez (2016). Repeat storm surge disasters of Typhoon Haiyan and its 1897 predecessor in the Philippines, *Bulletin of the American Meteorological Society* **97**, no. 1, 31-48.
- Stuiver, M., P.J. Reimer, and R.W. Reimer (2020). CALIB 8.2 [WWW program] at <http://calib.org>, accessed 2020-12-26.
- ten Brink, U. (2005). Vertical motions of the Puerto Rico Trench and Puerto Rico and their cause, *J. Geophys. Res.* **110**, no. B6.
- ten Brink, U. S., J. D. Chaytor, E. L. Geist, D. S. Brothers, and B. D. Andrews (2014). Assessment of tsunami hazard to the U.S. Atlantic margin, *Mar. Geol.* **353**, 31-54.
- Tuttle, M. P., A. Ruffman, T. Anderson, and H. Jeter (2004). Distinguishing tsunami from storm deposits in Eastern North America: The 1929 Grand Banks Tsunami versus the 1991 Halloween Storm, *Seismol. Res. Lett.* **75**, no. 1, 117-131.
- Tuttle, M., Z. Fuentes, and W. Schmidt (2017). Paleotsunami record of large offshore earthquakes north of Puerto Rico and the U.S. Virgin Islands, Final Technical Report, Prepared for U.S. Geological Survey grant G12AP20000, 40 p.
- von Hillebrandt-Andrade, C. (2013). Minimizing Caribbean Tsunami Risk, *Science* **341**, no. 6149, 966.
- Wei, Y., U. ten Brink, B. F. Atwater, M. P. Tuttle, R. B Halley, N. Feuillet, J. Accardo, and Z. Fuentes (2012). Near-field tsunami inferred from numerical modeling of medieval overwash at Anegada, British Virgin Islands, 2012 Fall Meeting, AGU, San Francisco, California, 3–7 December.
- Wei, Y., B. F. Atwater, U. ten Brink, and V. Roeber (2016). Exploring the cause of catastrophic Caribbean inundation in 1200-1480 C.E. using numerical models compared with geological evidence, Abstract NH51D-03, 2016 Fall Meeting, AGU, San Francisco, California, 11-15 December.

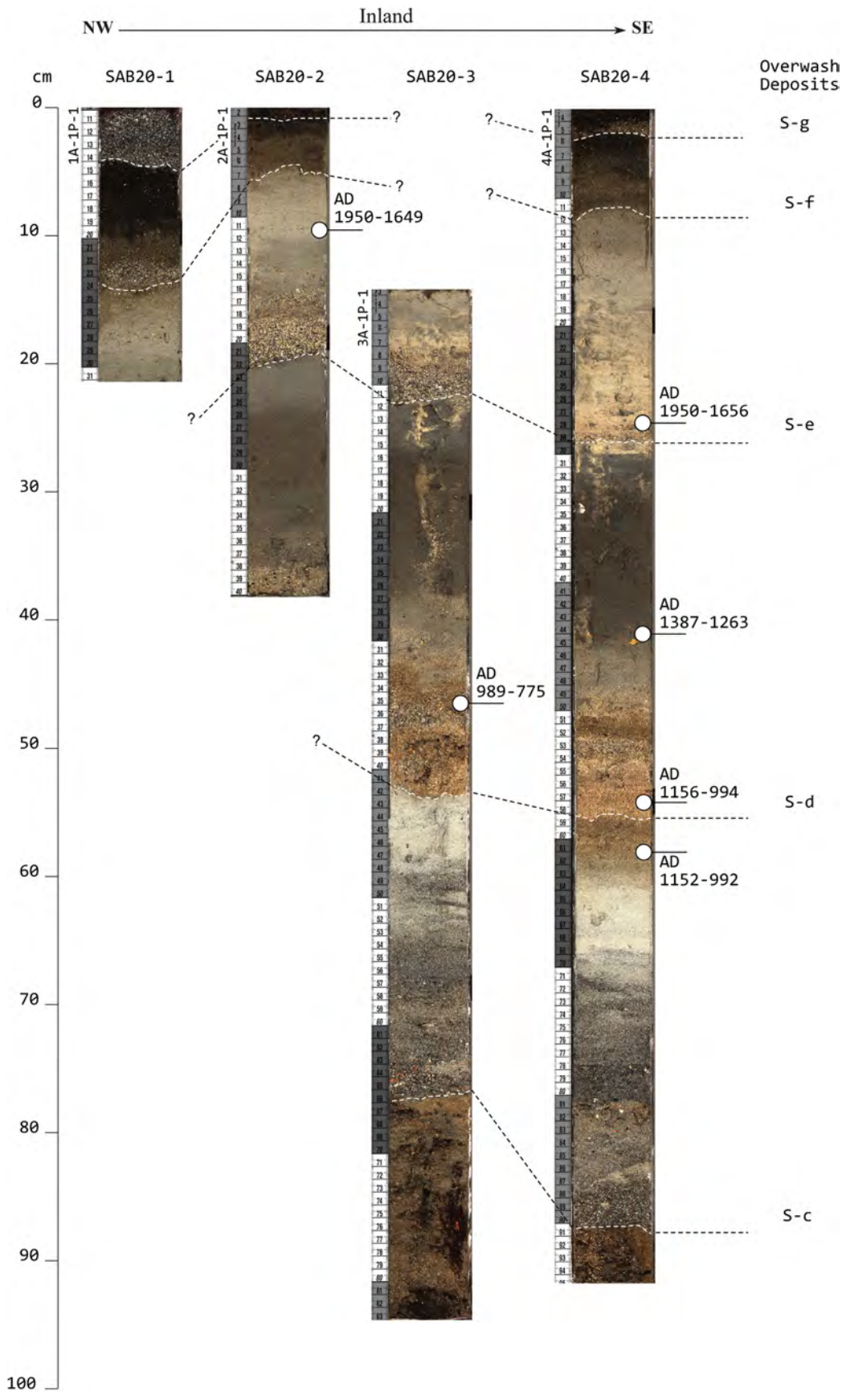
BIBLIOGRAPHY

- Fuentes, Z., M. Tuttle, and W. Schmidt (2012). Overwash deposits from the past 3,000 years on St. Thomas, U.S. Virgin Islands, *Geological Society of America*, Abstracts with Programs, v. 42, n. 5, p. 460.
- Fuentes, Z., M. P. Tuttle, and W. Schmidt (2016). Ecological changes and overwash events at three coastal ponds of St. Thomas, U.S. Virgin Islands, in Proceedings II General Assembly of the Latin America and Caribbean Seismological Commission (LACSC), San José, Costa Rica.

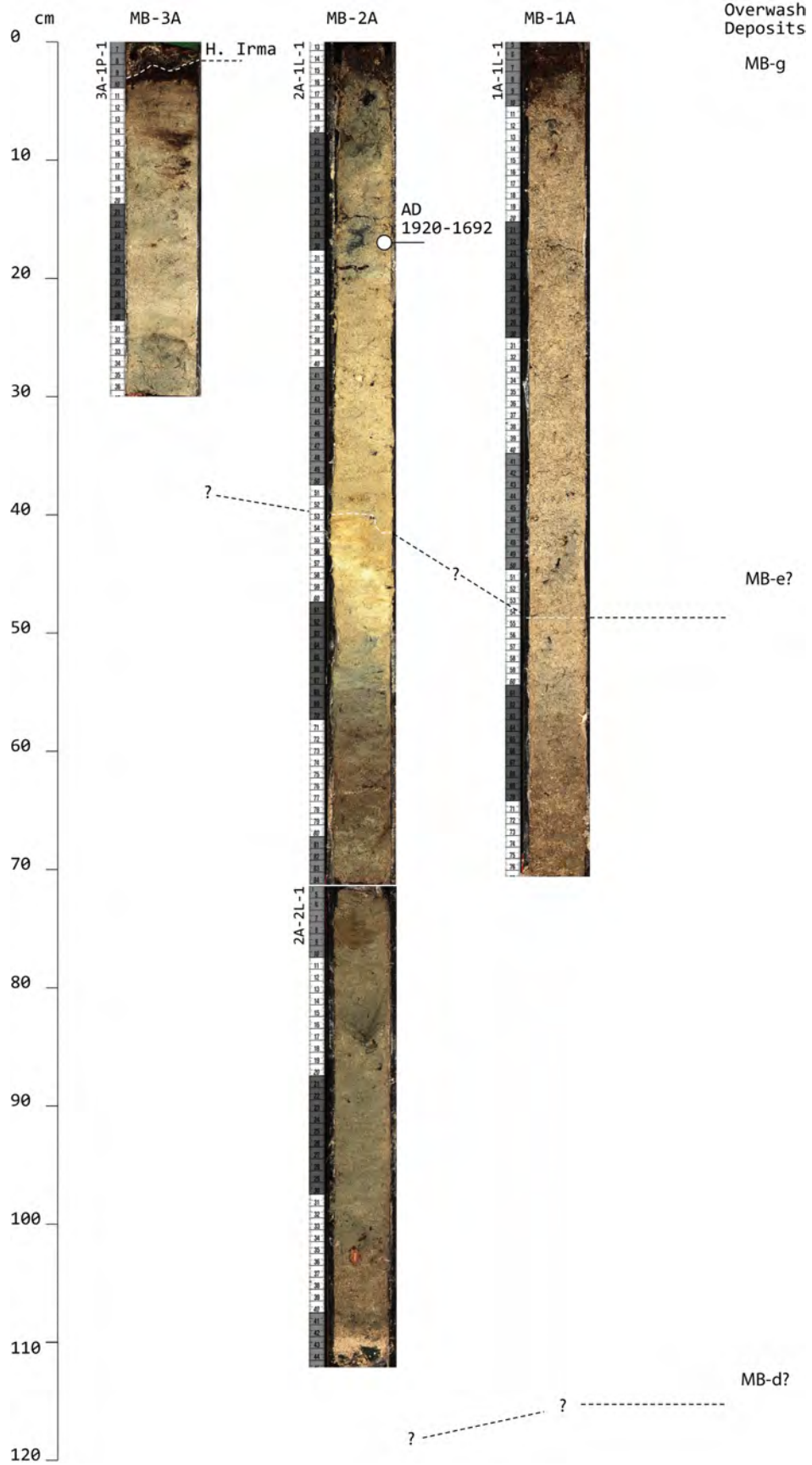
- Tuttle, M., Z. Fuentes, and W. Schmidt (2017). Paleotsunami record of large offshore earthquakes north of Puerto Rico and the U.S. Virgin Islands, Final Technical Report, Prepared for U.S. Geological Survey grant G12AP20000, 40 p.
- Fuentes, Z., M. Tuttle, and W. Schmidt (2017). Sand scripts of past tsunamis in coastal ponds of St. Thomas, U.S. Virgin Islands, *Seismological Research Letters*, doi: 10.1785/0220170038.
- Fuentes, Z., M. P. Tuttle, and W. E. Schmidt (2020). Mid- to Late Holocene ecological changes and overwash events at three coastal ponds on St. Thomas, U.S. Virgin Islands, submitted to *Seismological Research Letters*, in revision.

APPENDIX

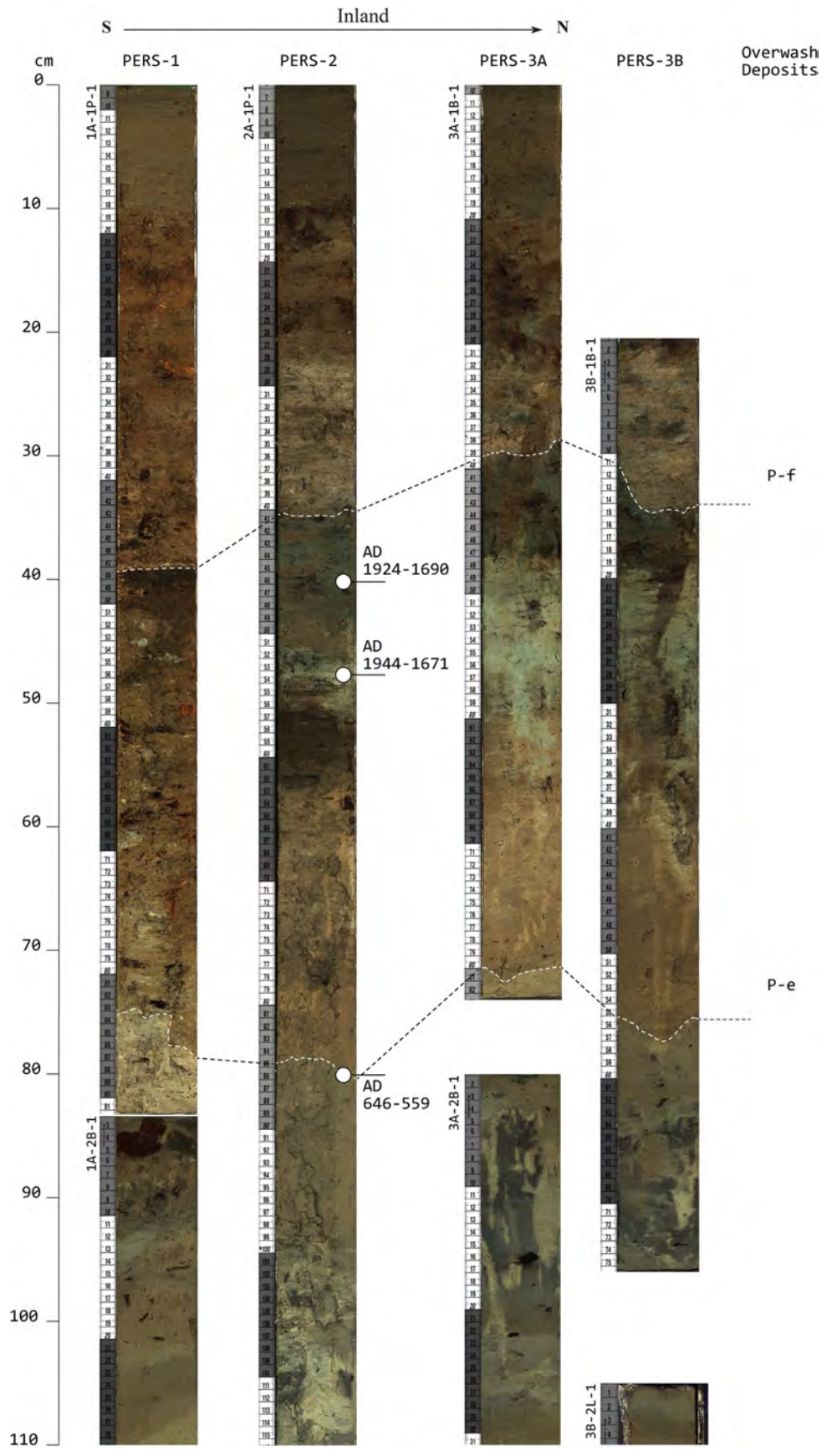
Cores Collected at Saba Pond in 2020

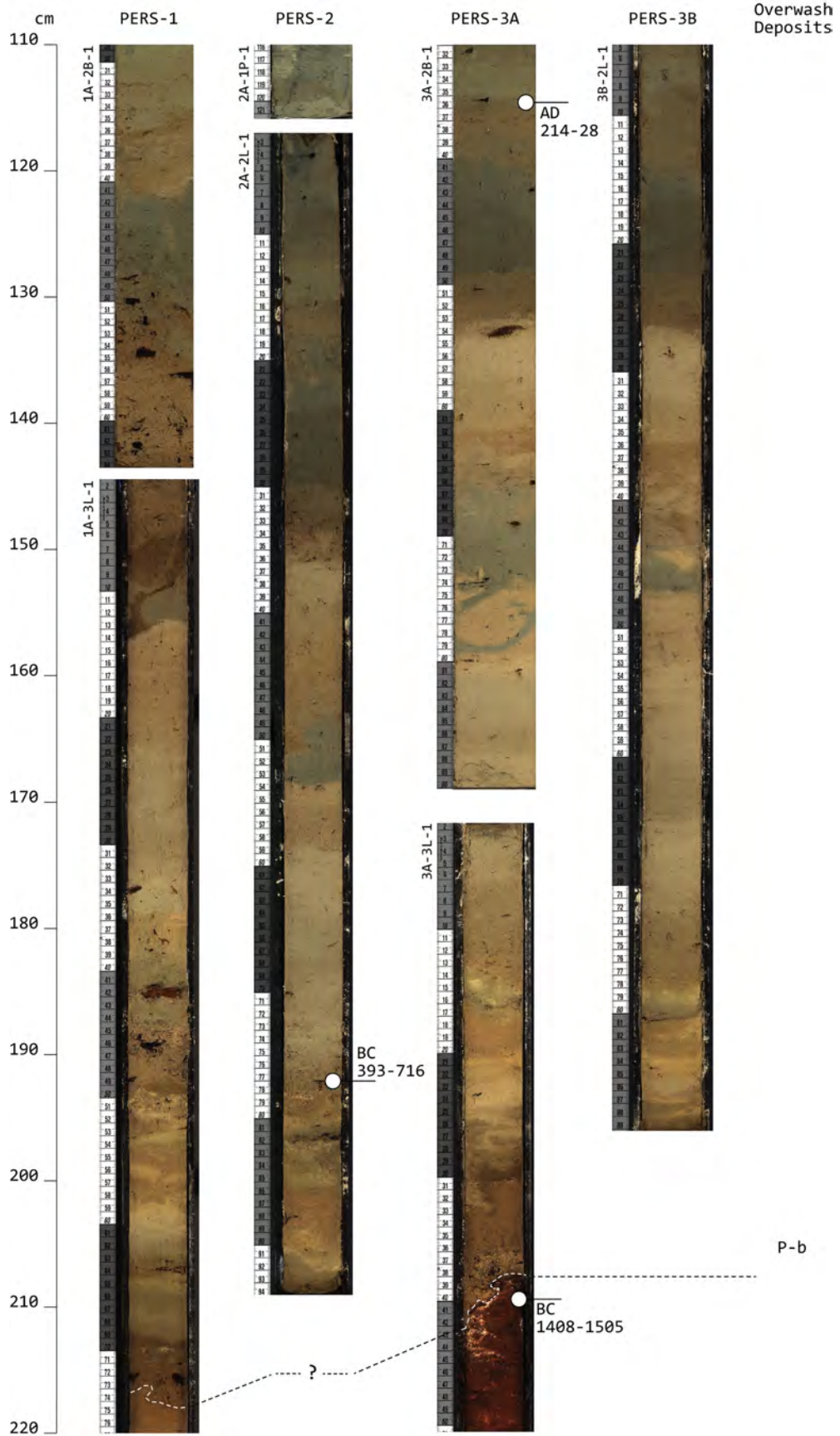


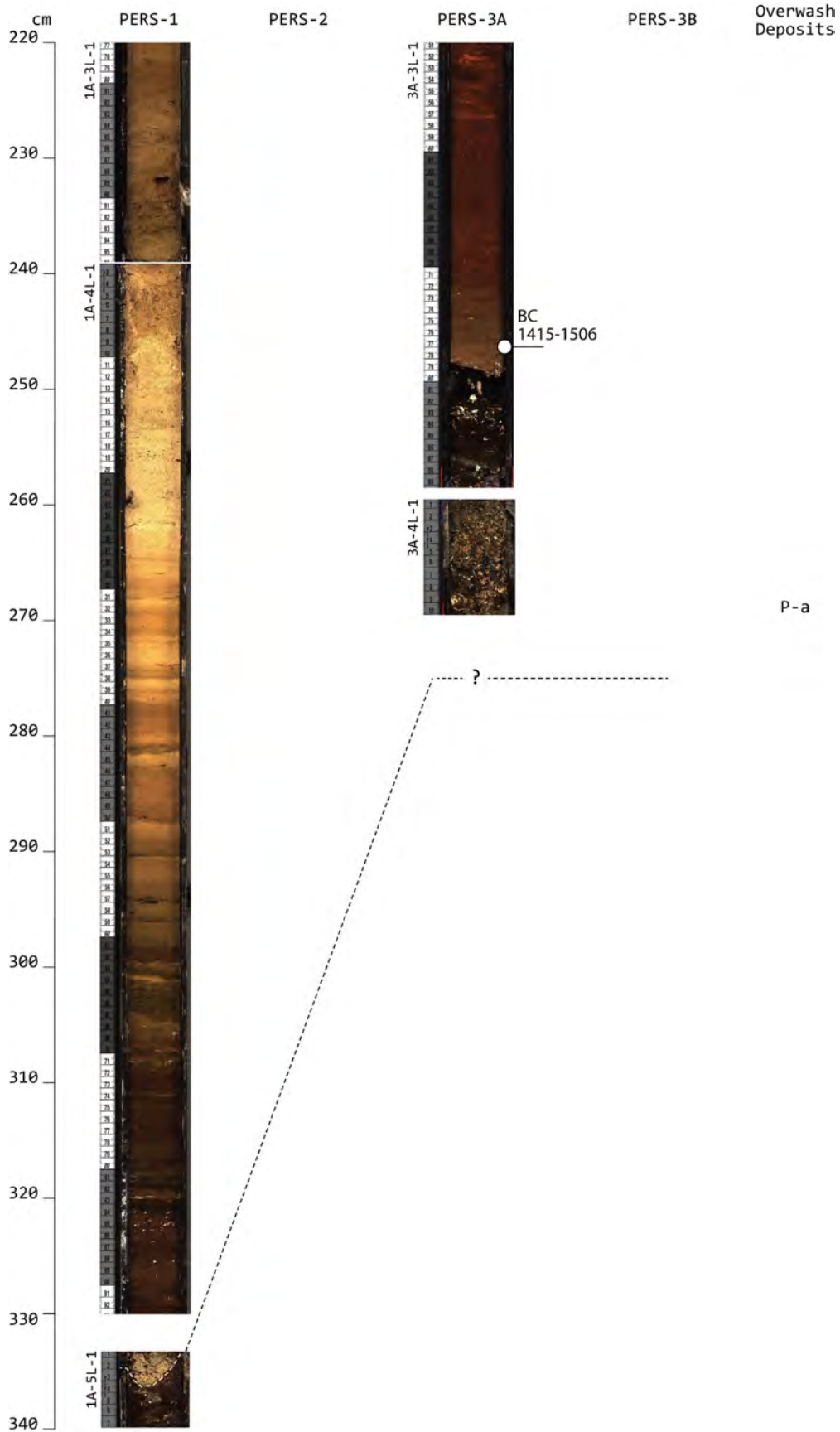
Cores Collected at Magens Bay in 2020



Cores Collected at Perseverance Pond in 2014







Cores Collected at Cabrita Pond in 2014

